ALMA MATER STUDIORUM
UNIVERSITÀ DI BOLOGNA

DOTTORATO DI RICERCA IN

SCIENZE BIOMEDICHE E NEUROMOTORIE

Ciclo 37

Settore Concorsuale: 06/D6 - NEUROLOGIA

Settore Scientifico Disciplinare: MED/26 - NEUROLOGIA

CYTOKINE STORM-ASSOCIATED ENCEPHALOPATHIES

Presentata da: Lorenzo Muccioli

Coordinatore Dottorato

Matilde Yung Follo

Supervisore

Francesca Bisulli

Co-supervisore

Maria Guarino

Esame finale anno 2025

SUMMARY

ABSTRACT

Background and Aims: Cytokine storm-associated encephalopathies arise in response to severe inflammatory conditions and include neurotoxicity related to CAR-T cell therapy (ICANS), neuro-COVID, and febrile infection-related epilepsy syndrome (FIRES). This PhD research explores key biomarkers and clinical manifestations associated with each of these disorders, focusing on the roles of EEG in predicting ICANS, S100B and neurofilament light chain (NfL) in neuro-COVID, and anatomo-electroclinical features in FIRES.

Methods: a prospective cohort of CAR-T recipients was assessed with a standardized protocol, involving EEGs recorded before and after infusion to investigate their predictive value for ICANS. For neuro-COVID, S100B and NfL serum levels were analyzed in COVID-19 patients with and without neurological symptoms to assess their diagnostic and prognostic utility. FIRES cases were evaluated to characterize clinical and investigative features.

Results: among 68 CAR-T therapy patients, 22 (32%) developed ICANS, the majority of whom had features consistent with a frontal-lobe encephalopathy; two died due to fulminant cerebral edema. EEG abnormalities, particularly theta and delta slowing, were predictive of ICANS. In 279 COVID-19 patients, elevated NfL levels corresponded with Neuro-COVID disease severity, whereas S100B results were less consistent. Four FIRES patients had anatomo-electroclinical features consistent with neuroinflammation and was associated with secondary sclerosing cholangitis in critically ill patients.

Discussion: this research highlights the significance of identifying biomarkers and electroclinical features in cytokine storm-associated encephalopathies and lays the groundwork for translational studies aiming to apply diagnostic and therapeutic findings across these syndromes. Future research should prioritize validation of multi-biomarker panels and cross-condition comparisons.

LIST OF ABBREVIATIONS

ACNS: American clinical neurophysiology society

ASM: antiseizure medication

BBB: blood-brain-barrier

CAR: chimeric antigen receptor

CI: confidence interval

CORE: COVID-19-related encephalopathy

CRP: C-reactive protein

CRS: cytokine release syndrome

CySE: cytokine storm-associated encephalopathy

DILI: drug-induced liver injury

DLBL: diffuse large B-cell lymphoma

EA: epileptiform abnormalities

FIRES: febrile infection-related epilepsy syndrome

ICANS: immune effector cell-associated neurotoxicity syndrome

ICU: intensive care unit

IQR: interquartile range

IVIg: intravenous immunoglobulin

MCL: mantle cell lymphoma

mRS: modified Rankin scale

MV: mechanical ventilation

OR: odds ratio

NEA: non-epileptiform abnormalities

NfL: neurofilament light chain

NORSE: new-onset refractory status epilepticus

SE: status epilepticus

PBF: predominant background frequency

PDR: posterior dominant rhythm

PMBCL: primary mediastinal B-cell lymphoma

SC: state changes

INTRODUCTION

The cytokine storm umbrella encompasses several disorders at the intersection of hematology, oncology, rheumatology, and virology. Cytokine storm is characterized by a dysregulated immune response to various triggers and is defined by elevated circulating cytokine levels, acute systemic inflammatory symptoms, and secondary organ dysfunction, including the brain (Fajgenbaum et al., 2020). Activated macrophages and monocytes appear to be responsible for the pathological hyperinflammation, regardless of the triggers (Fajgenbaum et al., 2020). Several cytokine storm disorders have been described, including COVID-19-associated cytokine storm (Webb et al. 2020), cytokine release syndrome due to chimeric antigen receptor (CAR) T-cell therapy (Lee et al., 2019), hemophagocytic lymphohistiocytosis (Brisse et al., 2015), macrophage activation syndrome (Ravelli et al. 2016), and multicentric Castleman disease (Fajgenbaum et al., 2017).[6] Although their *primum movens* differ, they share several laboratory abnormalities and clinical features, notably encephalopathy (Fajgenbaum et al., 2020; Webb et al., 2020; Pensato et al., 2021). Similar clinical and investigative findings have been reported in other encephalopathies associated with hyperinflammation, such as febrile infection-related epilepsy syndrome (FIRES) (Wickstrom et al., 2022). Considering the shared pathophysiological and anatomo-electro-clinical features between encephalopathies developing in this hyperinflammatory context, the unifying definition of cytokine storm-associated encephalopathy (CySE) has been proposed (Pensato et al., 2021). The following sections will analyze the main characteristics of three cytokine storm-associated neurological disorders (neurotoxicity associated with CAR-T therapy, neuro-COVID, and FIRES), focusing on the background elements relevant for the research that has been conducted in this PhD project.

Neurotoxicity associated with CAR-T therapy

CAR T-cell therapy is a novel and highly effective treatment for refractory hematological malignancies, notably B-cell non-Hodgkin lymphoma (Sterner et al., 2021). Unfortunately, its therapeutic benefit is limited by treatment-related toxicities, namely cytokine release syndrome (CRS) and immune effector cell-associated

neurotoxicity syndrome (ICANS) (Morris et al., 2022). CRS is a well-known cytokine storm disorder that results from the large amount of cytokines released from engaged immune cells and usually presents with fever, hypoxia, and hypotension, potentially leading to multiorgan failure (Neelapu et al., 2018). ICANS has a reported incidence ranging from 37.5% to 77% and a mortality rate of 3% (Grant et al., 2022). Its pathogenesis is strictly linked to CRS, which contributes to blood-brain barrier (BBB) damage and subsequent transmigration of proinflammatory products into the central nervous system (Gust et al., 2017; Morris et al., 2022). Some recurrent clinical features have been observed, typically involving encephalopathy variably associated with language disturbances, other focal neurological deficits, tremor, and seizures (Rubin et al., 2019). The treatment of ICANS is based on its severity and consists of corticosteroids, associated with anti-cytokine drugs such as anakinra or siltuximab for steroid-refractory ICANS. While several studies on ICANS have been conducted, comprehensive prospective real-world evaluations are still lacking.

ICANS Prediction and EEG

In addition to CRS, other factors increasing the risk of developing ICANS include elevated serum levels of C-reactive protein (CRP) and ferritin, lymphoma type, and the specific CAR T-cell product (Karschnia et al., 2019; Lee et al., 2019; Rubin et al., 2020; Butt et al., 2023).

A timely identification of neurotoxicity is essential for enabling prompt intervention with immunomodulatory treatments to prevent clinical deterioration (Neelapu et al., 2018). However, the opportunity to prevent ICANS using prophylactic treatments is currently under investigation and preliminary evidence on the efficacy of anakinra is already available from non-randomized studies (Park et al., 2023; Strati et al. 2023). In this context, predictive biomarkers would refine the selection of patients who may benefit from the prophylactic treatment. Nevertheless, the prediction of ICANS development remains, at present, a pressing unmet clinical need. EEG is a widely available, non-invasive, and cost-effective technique, highly sensible in evaluating patients with encephalopathy, regardless of the etiology (Ponten et al., 2023), thus representing a candidate biomarker for ICANS.

Studies investigating EEG changes during ICANS revealed significant alterations such as diffuse background slowing, rhythmic delta activity, sporadic and epileptiform discharges, supporting its diagnostic role (Herlopian et al., 2018; Beuchat et al., 2022; Huby et al., 2023). On the other hand, there is a lack on EEG performed before CAR T-cell infusion and, even more notably, on EEGs performed following the infusion prior to the onset of ICANS, as EEGs are not routinely performed in this setting.

Neurological manifestations of COVID-19

COVID-19 is a pandemic caused by severe acute respiratory syndrome coronavirus 2 (SARS-CoV-2). The condition encompasses a broad spectrum of severity, associated in a subgroup of patients with cytokine storm (Webb et al., 2020). Since the beginning of the pandemic, it was evident that COVID-19 does not only affect the respiratory system, as other organs are targeted by the virus or sensitive to adaptive changes following infection. In particular, virus-related neurological manifestations have been reported (neuro-COVID). These can be divided into acute (Beghi et al., 2023), occurring during the active infection by the virus, or delayed after the viral infection ceases (Taruffi et al., 2023; Beretta et al., 2023).

The features of neuro-COVID have been described in several publications (reviewed in Cho et al., 2023; Ousseiran et al., 2023). However, most available data were gathered by inhomogeneous approaches (single centers, small and selected samples, case reports) and in heterogeneous populations. Furthermore, published studies often adopted different diagnostic criteria and assessment of the course of the disease (Beghi et al., 2021). Thus, a literature survey does not allow for a reproducible strategy to assess disease severity and neuro-COVID risk.

Neurological complications of COVID-19 include encephalopathies, stroke, seizures and status epilepticus, myelitis, cranial and peripheral neuropathies, and myopathies (Cho et al., 2023; Ousseiran et al., 2023). Although neuro-COVID and specifically COVID19-related encephalopathy (CORE) was initially attributed to CNS invasion by SARS-CoV-2, based on evidence from other coronaviruses neuroinvasive and neurotropic properties, SARS-CoV-2 RNA is almost invariably undetectable in the CSF of patients with neurological manifestations (Solomon et al., 2021). Additionally,

CSF analysis, neuroimaging, and neuropathological findings, as well as the clinical response to various immunotherapies, are not consistent with an infectious disease targeting the brain but rather with an immune-mediated pathogenesis (Remsik et al., 2021; Pensato et al., 2021). Therefore, a cytokine-mediated neuroinflammatory process, associated with cytokine storm, has been suggested as the underlying pathogenic mechanism for CORE (Muccioli et al., 2020; Remsik et al., 2021; Pensato et al., 2021). Cytokine storm-associated immunothrombosis arguably plays a role also in other complications of COVID-19, notably stroke (Solomon et al., 2021; Pensato et al., 2023). In Neuro-COVID patients, similarly to ICANS, BBB disruption has been implicated in the pathogenesis, and is demonstrated by the observation of elevated albumin levels in the CSF (MacLean et al., 2020; Alquisiras-Burgos et al., 2021; Perrin et al., 2021). In vitro models also revealed that the BBB can be disrupted by the virus (Buzhdygan et al., 2020).

S100B and Neurofilament light chain

The astrocytic protein S100B has been widely recognized as a marker of BBB integrity. It levels in serum correlate with albumin coefficients, brain CT and MRI enhancement (Blyth et al., 2009; Marchi et al., 2007). Its negative predictive value for many neurological conditions has been diagnostically exploited for many years, and its use as a prognostic marker in TBI is used in Scandinavian countries as a surrogate to CT scans (Unden et al., 2005). Others have shown that S100B was found elevated in the blood of COVID-19 patients (Perrin et al., 2020) and correlated with disease severity (Aceti et al., 2020). Taken together, these data suggest that monitoring BBB function in COVID-19 patients may be helpful in pursuing neurological complications in a timely manner.

However, the data using S100B to predict COVID-19 or to classify disease severity are contradictory. In an early study, a positive correlation between S100B and disease severity was shown (Aceti et al., 2020), but others found no correlation (Sahin et al., 2022). An additional peripheral biomarker has been proposed as a prognostic tool in neuro-COVID, namely the neurofilament light chain (NfL) (Hay et al., 2021). NfL is a marker of neuroaxonal injury used in various neurological disorders, typically for prognostic or staging purposes (Wang et al., 2019; Freedman et al., 2024). NfL was

found elevated in neuro-COVID in a few studies (Needham et al., 2021; Zingaropoli et al., 2022), while others found no correlation (Sahin et al., 2022).

A recurring motif across all biomarker studies centered on establishing correlations between biomarker levels and either disease severity or the manifestation of neuro-COVID. However, due to the aforementioned reasons, the results were largely inconclusive.

Febrile infection-related epilepsy syndrome (FIRES)

Febrile infection-related epilepsy syndrome (FIRES) is a rare and devastating condition considered a subcategory of new-onset refractory status epilepticus (NORSE), i.e. a de novo onset of refractory status epilepticus (RSE) without an identifiable acute or active structural, toxic, or metabolic cause (Hirsch et al., 2018). The FIRES diagnosis requires a prior febrile illness starting between two weeks and 24 hours before the onset of SE (Hirsch et al., 2018). If no explanation for the clinical presentation of NORSE is found, it is considered cryptogenic NORSE (or NORSE of unknown etiology). Of note, the presence of prodromal high fever of unknown origin before the onset of SE was found as a predictive factor for cryptogenic NORSE (Yanagida et al., 2020). The pathogenesis of FIRES involves a dysregulated systemic inflammatory response (i.e., cytokine storm) following infection, which can result in blood-brain-barrier dysfunction and trigger an uncontrolled cytokine-mediated neuroinflammatory cascade, promoting the development of seizures and their refractoriness (Wickstrom et al., 2022). The exaggerated response to an infection as the trigger of a cytokine storm disorder is similar to what happens for COVID-19 or some cases of hemophagocytic lymphohistiocytosis.

Patients with FIRES commonly have T2/FLAIR hyperintensities in the mesial temporal lobe and other brain structures, notably the claustrum in adult patients (so-called “claustrum sign”) (Meletti et al., 2015). Notably, this latter finding is frequently encountered also in familial acute necrotizing encephalopathy, another life-threatening febrile infection-related encephalopathy disorder occurring in children, and has been reported in CORE and ICANS (Neilson et al. 2009; Zuhorn et al., 2020; Santomasso et al., 2018).

Patients with FIRES typically have an aggressive refractory form of convulsive SE, requiring treatment with multiple lines of antiseizure medications and anesthetics, and prolonged hospitalization in the intensive care unit (ICU). As immunological activation is likely, first-line immunotherapy should be considered within 72 hours of seizure onset in cryptogenic cases (Wickstrom et al., 2022). Pulse steroids and intravenous immunoglobulin (IVIg) should be administered as the first lines of therapy. In cryptogenic FIRES without clear features of autoimmune encephalitis, IL-1 receptor antagonists (anakinra) or IL-6 antagonists (tocilizumab or siltuximab) should be initiated (Wickstrom et al., 2022). Concerning the outcomes and the chronic phase, about 80% of patients develop chronic epilepsy (Meletti et al., 2017). Most patients need to undertake an intensive program of motor and cognitive rehabilitation, combined with social service interventions to promote social activities, return to school or work, and quality of life of the patients and their families (Wickstrom et al., 2022).

Due to the rarity of the disease, continuous efforts are essential to understand the mechanisms of FIRES and to improve diagnosis and treatment.

AIMS

The overall aim of this project was to describe the features of cytokine storm-associated neurological disorders, focusing on the following three aims:

AIM 1: to describe the anatomo-electroclinical features of ICANS and study the role of EEG as a predictive biomarker of ICANS development in recipients of CD19-directed CAR-T therapy.

AIM 2: to evaluate the possible diagnostic and prognostic roles of serum biomarkers in COVID-19, namely S100B and NfL, with specific emphasis on their ability to predict disease severity and neurological involvement.

AIM 3: to describe the anatomo-electroclinical features of FIRES and enucleate novel characteristics of this condition.

AIM 1: Neurotoxicity associated with CAR-T therapy

Methods

Setting and population

In this monocentric, prospective, real-life cohort study, all consecutive patients with large B-cell non-Hodgkin lymphoma (diffuse large B-cell lymphoma [DLBCL] and primary mediastinal B-cell lymphoma [PMBCL]) and mantle cell lymphoma (MCL) receiving an anti-CD19 CAR T-cell product at the Institute of Hematology "L. e A. Seragnoli", IRCCS Azienda Ospedaliero-Universitaria di Bologna, Italy, between August 2019 and September 2022 were recruited. Detailed hematological inclusion criteria, defined by the Italian Medicine Agency reimbursement criteria, included: (i) age between 18 and 70 years; (ii) Eastern Cooperative Oncology Group Performance Status (ECOG PS) ≤ 1; (iii) diagnosis of large B-cell non-Hodgkin lymphoma (DLBCL, PMBCL) or MCL relapsed after or refractory to at least two prior specific lines of treatment; (iv) no CNS involvement, and (v) an adequate organ function.

Patients with large B-cell lymphoma (DLBCL and PMBCL) received one of the two approved CD-19 targeted CAR T-cell therapy (axicabtagene ciloleucel [axi-cel] or tisagenlecleucel [tisa-cel]) based on slot production availability and histology, while patients patients with MCL received brexucabtagene autoleucel (brexu-cel). All patients received lymphodepleting chemotherapy (cyclophosphamide 250–500 mg/m2 plus fludarabine 25–30 mg/m2) for three consecutive days, starting five days before CAR T-cells infusion. After leukapheresis, a subset of patients underwent bridging therapy to control the disease while waiting to infuse CAR T-cells. The most commonly used bridging treatments were chemotherapy, radiotherapy, corticosteroids, or immunotherapy at the discretion of the treating hematologist.

Neurological assessment protocol

All patients underwent a standardized neurological protocol, including neurological evaluation at baseline and during the hospital stay for CAR T-cell treatment. All neurological examinations were performed by certified neurologists who received specific training in the assessment of CAR-T-related neurotoxicity and always included the ICE (immune effector cell-associated encephalopathy) score (Lee et al., 2019). The baseline evaluation was performed 15–30 days before the day of CAR T-

cells infusion (day 0) and included neurological examination, EEG, brain MRI and neuropsychological assessment. Concomitantly, patients were started on prophylactic antiseizure medication (levetiracetam 1500 mg/die) following the CAR T-cell therapy-associated TOXicity (CARTOX) Working Group recommendation (Neelapu et al., 2018). The anti-seizure medication was then gradually tapered and discontinued within one month after hospital discharge. From day 0, patients underwent regular in-hospital neurological examinations and EEG studies to monitor the development of neurotoxicity (specifically at days + 1, + 3, + 7, + 10, and + 14 from CAR T-cells infusion and before discharge). In the presence of ICANS, daily neurological examination and further diagnostic tests guided by neurological manifestations were performed, such as repeated EEG or brain CT/MRI. Treatment was based on ICANS severity and consisted of corticosteroids, associated with siltuximab or anakinra for steroid-refractory ICANS.

At baseline, demographic and clinical data were collected, including age, sex, comorbidities, blood test results, lymphoma characteristics, and previous failed treatments. According to the Ann Arbor/Cotswolds classification, at apheresis, patients were staged and classified as having early (stage I–II) or advanced (stage III–IV) stage disease (Lister et al., 1989). CRS and ICANS were assessed and graded based on the American Society for Transplantation and Cellular Therapy (ASTCT) Consensus published (Lee et al., 2019) (Tables 1 and 2). CRS grading was assigned by the inpatient attending hematologist, while the treating neurologist always confirmed ICANS grading.

Table 1: American Society for Transplantation and Cellular Therapy (ASTCT) CRS Consensus Grading for Adults (Lee et al., 2019)

CRS Parameter	Grade 1	Grade 2	Grade 3	Grade 4
Fever[*]	Temperature ≥38°C	Temperature ≥38°C	Temperature ≥38°C	Temperature ≥38°C
		With		
Hypotension	None	Not requiring vasopressors	Requiring a vasopressor with or without vasopressin	Requiring multiple vasopressors (excluding vasopressin)
		And/or[†]		
Hypoxia	None	Requiring low-flow nasal cannula[‡] or blow-by	Requiring high-flow nasal cannula[‡], facemask, nonrebreather mask, or Venturi mask	Requiring positive pressure (eg, CPAP, BiPAP, intubation and mechanical ventilation)

Table 2. ASTCT ICANS Consensus Grading for Adults (Lee et al., 2019)

Neurotoxicity Domain	Grade 1	Grade 2	Grade 3	Grade 4
ICE score*	7-9	3-6	0-2	0 (patient is unarousable and unable to perform ICE)
Depressed level of consciousness†	Awakens spontaneously	Awakens to voice	Awakens only to tactile stimulus	Patient is unarousable or requires vigorous or repetitive tactile stimuli to arouse. Stupor or coma
Seizure	N/A	N/A	Any clinical seizure focal or generalized that resolves rapidly or nonconvulsive seizures on EEG that resolve with intervention	Life-threatening prolonged seizure (>5 min); or Repetitive clinical or electrical seizures without return to baseline in between
Motor findings‡	N/A	N/A	N/A	Deep focal motor weakness such as hemiparesis or paraparesis
Elevated ICP/ cerebral edema	N/A	N/A	Focal/local edema on neuroimaging§	Diffuse cerebral edema on neuroimaging; decerebrate or decorticate posturing; or cranial nerve VI palsy; or papilledema; or Cushing's triad

EEG as a predictive biomarker

To study the predictive role of EEG, We included patients with availability of: (i) at least the baseline EEG record, (ii) neurologic examination and ICANS score at the time of EEG recording. EEGs were excluded from analysis if excessive artifacts prevented their reliable evaluation.

Routine EEGs were recorded using the standard international 10–20 system for electrodes placement. A bipolar montage, 50 Hz notch filters and 0.5–40 Hz bandpass filters were applied. In the intensive care unit (ICU) setting, EEGs were recorded after the temporary discontinuation of anesthetics. The included records were analysed qualitatively and quantitatively.

Qualitative evaluation

The records have been visually assessed independently by two expert neurophysiologists who were blinded to patients' histories and not involved in the neurological assessment of CAR T-cell therapy recipients.

The American Clinical Neurophysiology Society's (ACNS) Standardized Critical Care EEG Terminology (Hirsch et al., 2021) was applied, with certain terms adapted to accommodate the distinct setting in which EEGs were conducted, taking into account the variations between prolonged monitoring in the ICU and routine EEG recordings.

To facilitate the process, an ad hoc EEG evaluation form has been created, containing the following sections for each record:

- Background activity (BA) (alternative options in square brackets)

  - Symmetry [present/absent];

  - Predominant Background Frequency (PBF) [beta/alpha/theta/delta];

  - Posterior Dominant Rhythm (PDR) [present/absent];

  - Reactivity [present/absent];

  - Voltage [normal/attenuated/suppressed];

  - State changes (SC) [absent/normal features/pathological features]*.

- Non-epileptiform abnormalities (NEA)

  Focal or diffuse sporadic slowing, in theta or delta frequency.

- Epileptiform abnormalities (EA)

  Spikes, polyspikes or sharp waves with or without triphasic morphology (both sporadic and periodic).

*State changes are defined in ACNS Terminology as different types of background activities related to the level of alertness or stimulation (Hirsch et al., 2021). In the present study, we defined state changes "pathological" if the posterior alpha rhythm was frequently replaced by long-lasting diffuse delta activity, rapidly emerging after eye-closure. This pattern differs from physiological vigilance fluctuations characterized by gradual alpha rhythm disappearance while theta activity emerges, usually after few minutes in a relaxed state with closed eyes.

An example is represented in the following Figure.

Figure 1. Example of pathological state changes on EEG

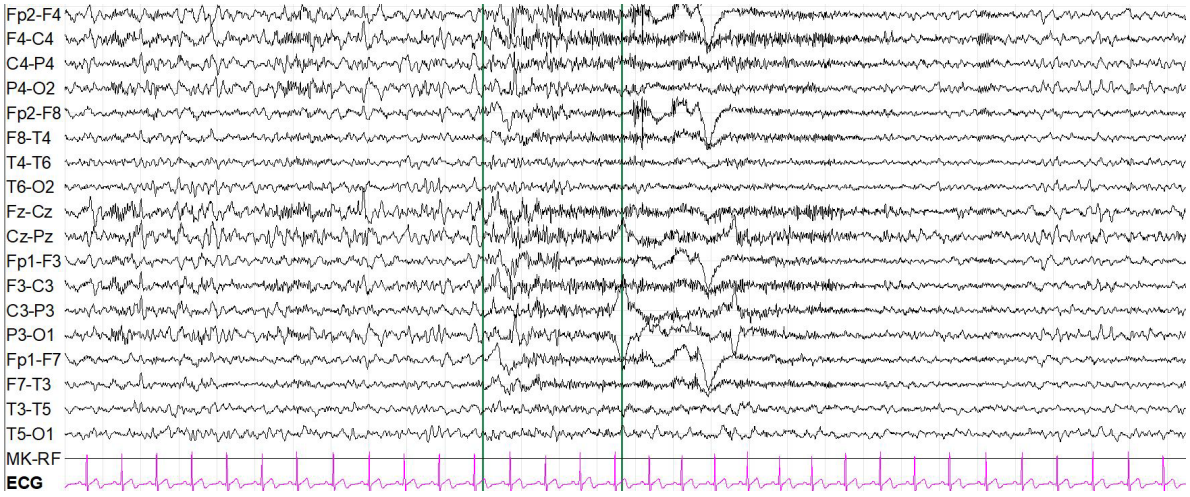

The prevalence of sporadic abnormalities (both NEA and EA) was defined as follows (correspondences with ACNS terminology in brackets):

- Low (corresponding to "occasional" and "rare"): < 1/minute.
- Moderate (corresponding to "frequent"): ≥1/minute but less than 1 per 10 seconds.
- High (corresponding to "abundant"): ≥1 per 10 seconds.

Then, each EEG has been assigned a final "grade" reflecting its overall significance, ranging from 0 (normal) to 3 (severely abnormal) (Table 3). In case of discrepancies, a definitive judgment was obtained by open debate among the two raters while keeping clinical outcomes hidden.

After completing the blind evaluation process, we selected the EEGs recorded prior to ICANS onset for comparison with those of non-ICANS patients.

Table 3. EEG Grading Scale

PBF	**Reactivity**	**Sporadic Theta**	**Sporadic Delta**	**State Changes**	**Epileptiform Abnormalities**	**Overall Significance**	**Grade**
Alfa/ Beta	Present	+	Absent	Absent/ Physiological	Absent	Normal	**0**
Alfa/ Beta	Present	++	+	Pathological	Absent	Slightly abnormal	**1**
Theta	Present/ absent	+++	++	Not relevant	+	Moderately abnormal	**2**
Delta	Present/ absent	Not relevant	+++	Not relevant	++/+++	Severely abnormal	**3**

0 = Normal PBF ± Low prevalence sporadic Theta and/or physiological state changes.
1= Normal PBF + Moderate prevalence sporadic Theta and/or Low prevalence sporadic Delta and/or pathological state changes.
2= Theta PBF and/or Absence of reactivity and/or Moderate prevalence sporadic Delta and/or Low prevalence epileptiform abnormalities.
3= Delta PBF and/or High prevalence sporadic Delta and/or Moderate/High prevalence epileptiform abnormalities.

Legend: PBF= predominant background frequency; + = low prevalence; ++ = moderate prevalence; +++ = high prevalence; NA= not applicable.

Quantitative evaluation

Quantitative features have been analysed in relation to the time of recording:

- Baseline EEG.
- Post-infusion EEGs (T1; T3; T7; T14): records prior to ICANS onset were selected for comparison with those of non-ICANS patients.

All the eligible records were segmented into artifact-free time windows, using Brain Vision Analyzer 2.2. A final epoch representative of each EEG was obtained by assembling the artifact-free time windows. Each epoch had a minimum duration of 20 seconds and was processed according to an *ad hoc* pipeline, written in Python[29], to extract quantitative features describing the characteristics of the signal both in the time and frequency domains.

At first, each epoch was segmented into overlapping time windows of duration T=2.0 s, considering Δt=0.25 s as a time shift between consecutive windows. Such a segmentation made it possible to obtain multiple samples of the same feature from each epoch, increasing the accuracy of the final measures. Hence, appropriate algorithms were implemented to derive the following features:

- The signal energy $E\omega(t)$ for a given frequency band ω, representing the strength of the oscillations included in such an interval; the bands considered for the analysis were delta δ=[2,4] Hz, theta θ=[4,8] Hz, alpha α=[8,14] Hz, and beta β=[14,30] Hz.
- The signal entropy $H(t)$ and fractal dimension $F(t)$, estimating the complexity of the signal in terms of amplitude and phase distribution.
- The phase transfer entropy $PTE(t)$ between the different EEG channels, denoting the influence that each channel exercises over the others.
- Graph-based measures, including the in/out-degree, the betweenness and eigenvector centrality, and the eccentricity of each EEG channel, as well as the diameter of the overall EEG signal.

To appreciate the time-dependent variations in parameters and allow inter-patients comparison, the features concerning post-infusion EEGs were normalized with respect to the baseline EEG.

Statistical analysis

In descriptive analysis, continuous variables have been summarized and presented through mean, standard deviation (SD) and range (min-max), categorical variables through absolute numbers (n) and percentages (%). For continuous variables the Mann-Whitney test was used to evaluate differences between two groups, while the Chi-square test was used for categorical variables. Associations between qualitative or quantitative assessments of EEG tracings (time dependent variables) and the development of ICANS (outcome - time to event) have been assessed through univariable and multivariable Cox regression models. Time to enter in the analysis was the day of infusion. For the time-dependent variables (qualitative and quantitative assessments of EEG records), the values were updated at each time-point (T1, T3, T7, T14). The role of any confounding factors (age, sex, clinical characteristics, therapy, etc.) has been considered in the models. The multivariable model was selected using a step-wise procedure using likelihood ratio test to select the best model. Results were presented with hazard ratios (HR) and 95% confidence intervals (95% CI). Cohen's kappa was used to evaluate the inter-rater reliability between two raters (FB, PT) for the qualitative EEG evaluation. Statistical analysis was performed using Stata SE 14.2.

Standard protocol approvals

The study was approved by the institutional review board Ethical Committee AVEC (protocol number: CE: 319/2021/Sper/AOUBo). Written informed consent was obtained from all enrolled patients, both for study participation and data publication.

Results

Population

A total of 68 patients affected by refractory/relapsed NH lymphoma underwent CAR T-cell therapy in the study period and were included in the study. The median age at the time of infusion was 55.2 years (SD ±14; range 19-70). Female sex prevalence was 20/68 (29.4%). Histology cancer subtypes comprehended DLBCL in 50/68 (73.5%), PMBCL in 8/68 (11.8%), MCL in 9/68 (13.2%) and FL in 1/68 (1.5%). The mean disease duration and number of previous treatments attempted were 51.1 months (SD ±60.2; range 5-264] and 2.9 (SD ±1.3; range 1-8) respectively. 52/68 (76.5%) patients had advanced stage cancer (III or IV). The administered CAR T-cell product was Axi-

cel in 31/68 (45.6%), Tisa-cel in 28/68 (41.2%) and Brexu-cel in 9/68 (13.2%). All the patients were administered anti-seizure prophylaxis (levetiracetam 750 mg BID), starting from 10 days before the infusion day. The baseline features of the cohort are summarized in the following Table.

Table 4. Population baseline features

	Total patients (n = 68)
Age (years) Mean, (SD) [range]	55 (±14) [19-70]
Female sex	20 (29.4%)
Histology	
DLBCL	50 (73.5%)
PMBCL	8 (11.8%)
MCL	9 (13.2%)
FL	1 (1.5%)
Bulky (>7cm)	32 (47.1%)
Disease status	
Early refractory	56 (82.4%)
Refractory	4 (5.9%)
Relapsed	10 (14.7%)
Bridge therapy	48 (70.6%)
Pembrolizumab	6 (8.8%)
Steroids	6 (8.8%)
Chemotherapy	25 (36.8%)
Radiotherapy	4 (5.9%)
Combinations	7 (10.3%)
Previous treatments (n) Mean, (SD) [range]	2.9 (±1.3) [1-8]
ASCT	23 (33.8%)
History of lymphoma (months) Mean, (SD) [range]	51.1 (±60.2) [5-264]
Disease stage III-IV	52 (76.5%)

Serum inflammatory markers	
IL-6 (pg/mL)	17.5 (±28.6) [0.2-7.6]
IL-10 (pg/mL)	9.5 (±27.2) [0-185]
IL-8 (pg/mL)	45 (±75.8) [5-574]
Ferritin (ng/mL)	564 (±1139.1) [11-6787]
CRP (mg/dL)	2.44 (±4.5) [0.1-19.2]
D-dimer (mg/L)	1.7 (±2.9) [0.2-7.3]
CAR T-cells product	
Axi-cel	31 (45.6%)
Tisa-cel	28 (41.2%)
Brexu-cel	9 (13.2%)

LEGEND: ASCT= autologous stem cell transplantation; DLBCL= Diffuse large B-cell lymphoma; PMBCL= Primary mediastinal B-cell lymphoma; MCL= Mantle cell lymphoma, FL= Follicular lymphoma.

Association between CRS-related variables and ICANS

Among the overall cohort, CRS occurred in 58/68 (85.3%), with a mean latency from the infusion (T0) of 2.4 days (SD ± 2.3; range 0-11). Maximum CRS grade was 3, observed in 6/58 (10.3%) patients. CRS resolved in a mean time of 5.7 days (SD ± 4.2; range 1-30).

CRS characteristics, tocilizumab posology and mean peak levels of the serum inflammatory markers in the post-infusion period differed significantly between patients with and without ICANS. An earlier, more severe, and longer CRS, use of tocilizumab and higher inflammatory markers levels were observed in ICANS patients, as shown in the following Table.

Table 5. Correlations between CRS-related variables and ICANS

	Total patients (n = 68)	ICANS		p-value
		YES (n= 22)	NO (n=46)	
CRS	58/68 (85.3%)	22/22 (100%)	36/46 (78.3%)	
Onset (T)	2.4 [0-11]	1.2 [0-4]	3.2 [0-11]	**0.001**
Severe CRS (≥3)	6/58 (10.3%)	6/22 (27.3%)	0/36 (0%)	**<0.001**
Duration (days)	5.8 [1-30]	7.7 [2-30]	4.75 [1-2]	**<0.001**
Tocilizumab (n) (mean, SD) [range]	1.6 (±1.4) [0-4]	2.4 (±1.1) [0-4]	1.3 (±1.3) [0-3]	**0.002**
Serum Inflammatory Markers Peaks (mean, SD) [range]				
IL-6 (pg/mL)	1511.5 (±1841.1) [4.7-6773]	2722.4 (±2093.3) [59-6773]	883.1 (±1338.4) [4.7-4899]	**<0.001**
IL-10 (pg/mL)	145.7 (±681.1) [1-5406]	405 (±1193.9) [4-5406]	24.7 (±29.4) [1-115]	**<0.001**
IL-8 (pg/mL)	429.3 (±710.7) [31-5000]	730.7 (±1085.7) [43-5000]	288.7 (±397.7) [31-2446]	**0.011**
Ferritin (ng/mL)	1771.4 (±2353.7) [22-7500]	3589.4 (±3101.8) [155-7500]	902 (±1222) [22-7500]	**0.002**
CRP (mg/dL)	12.8 (±10.0) [0.2-46.4]	18.5 (±11.1) [3.8-46.4]	8.8 (±7.4) [0.2-30.9]	**<0.001**
D-dimer (mg/L)	4.3 (±3.8) [0.2-7.2]	6.9 (±4.7) [0.4-7.2]	2.3 (±1.8) [0.2-6.6]	**<0.001**

ICANS features

Neurotoxicity manifested in 22/68 (32.4%) patients, with an average onset time of 5.7 days (range 0-15) following the infusion. Among those affected, 9/22 (40.9%) patients experienced severe ICANS (grade ≥3), of whom 3 deceased early (two for fulminant cerebral edema and one for systemic complications). ICANS manifestations were preceded by CRS. Epileptic events (isolated tonic-clonic seizure, n=2; non-convulsive status epilepticus, n=1) were observed in 3/22 patients, two of whom exhibited fulminant cerebral edema. Most patients exhibited symptoms consistent with frontal lobe dysfunction, including dysexecutive syndrome, and palygraphia. ICANS features are summarized in the following table.

Table 6. Features of the ICANS cohort

ICANS patients (n)	22/68 (32.4%)
Disease timing and grading	
Severe ICANS (≥3)	9/22 (40.9%)
Onset (T) (SD) [range]	5.5 (±3.7) [0-15]
Mean duration (days) (SD) [range]	10 (±12.2) [1-52]
Relationship with CRS	
CRS prior or concomitant to ICANS	22/22 (100%)
Mean time from CRS onset to ICANS onset (days) (SD) [range]	4.3 (±3.5) [0-14]
ICU	
ICU admission	11/22 (50.0%)
Length of stay (days) (SD) [range]	9.7 (± 6.9) [2-24]
Clinical features	
Seizures	2/22 (9.1%)
NCSE	1/22 (4.5%)
Frontal lobe dysfunction	16/22 (72.7%)
Ideo-motor slowing	20/22 (90.9%)
Coma	9/22 (40.9%)
Dysgraphia/palygraphia	9/22 (40.9%)
Neuroimaging findings	
Unremarkable	12/19 (63.2%)
Focal or diffuse cerebral edema	5/19 (26.3%)
Leptomeningeal enhancement	1/19 (5.2%)
Intracerebral hemorrhage	1/19 (5.2%)
Treatment	
None	2/22 (9.1%)
Steroids	10 (45.5%)
Anakinra	7 (31.8%)
Siltuximab	8 (36.4%)
Early neurotoxicity outcome	
Spontaneous resolution	2 (9.1%)
Resolution following immunotherapy	17 (77.3%)
Neurotoxicity-related death	2 (9.1%)
Systemic complications-related death	1 (4.5%)

Legend: ICU= Intensive Care Unit; NCSE= Non-Convulsive Status Epilepticus; SD= Standard deviation; T= days from the infusion.

Clinical Vignette: a patient with fulminant cerebral edema

A 35-year-old woman, affected by chemo-refractory primary mediastinal large B cell lymphoma, received CAR T-cell therapy at the IRCCS AOU Bologna. A comprehensive neurological screening evaluation (neurological examination, EEG, nerve conduction study, brain MRI and neuropsychological tests) was unremarkable. The patient received five cycles of pembrolizumab (the first before leukapheresis and the other four as bridging therapy) and lymphodepleting chemotherapy, prior administration of axicabtagene ciloleucel (Axi-cel; 2× 106 anti-CD19 CAR T-cells/kg). Twelve hours after CAR T-cells infusion, she developed a grade 1 CRS, which resulted refractory to tocilizumab given for three doses on days+2 and+3 post CAR T-cells infusion. Tocilizumab was started concomitantly with a slight increase of both IL-6 (34.9 pg/ml, normal value <5.9 pg/mL) and C-reactive protein (5.05 mg/dL, normal value <0.5 mg/dL) plasma level. A chest CT scan and several blood cultures, performed according to the internal protocol, excluded an infectious etiology. CRS did not progress to a higher grade and neurological evaluations were repeatedly unremarkable. Nonetheless, during the night between day+ 3 and + 4, she developed vomiting in addition to fever and, on the following morning, she presented with non-fluent expressive aphasia and myoclonic postural tremors (ICANS grade 2), becoming rapidly lethargic. Intravenous dexamethasone (10 mg/q6h) was promptly started and she was transferred to the intensive care unit, where she was sedated and intubated. Few hours later, following sedation weaning, the patient was comatose (GCS=7; E3, V1, M3) and her right pupil was fixed and dilated, yet the other brainstem refexes were preserved (ICANS grade 4). Diffuse slowing was observed at EEG, while laboratory blood tests showed a dramatic increase of IL-6 (2144 pg/mL) and D-dimer levels (12.14 mg/dL), yet other inflammatory markers were only slightly increased, such as C-reactive protein (9.50 mg/dL) and ferritin levels (134 ng/mL). Brain CT scan revealed diffuse cerebral edema (Figure 2).The patient was promptly managed with both pharmacologic and non-pharmacologic interventions, including intravenous methylprednisolone (1000 mg), hyperventilation, head and trunk elevation up to 30 degrees, hypertonic saline and mannitol. Ultimately, a ventriculostomy with intraventricular intracranial pressure monitoring was placed, showing an ICP of 90 mmHg. This remarkably elevated value raised suspicion of brain death, thus

postponing decompressive craniectomy until CT angiography that confirmed the absence of cerebral blood flow. Notably, during the venous phase of CTA, cerebral veins were not detectable, yet a mild homogeneous contrast opacifcation was observed in the dural venous conduits. Brain death occurred in less than 12 h since the onset of neurological deterioration. Her family declined autopsy.

Figure 2. Head CT signs of diffuse cerebral edema

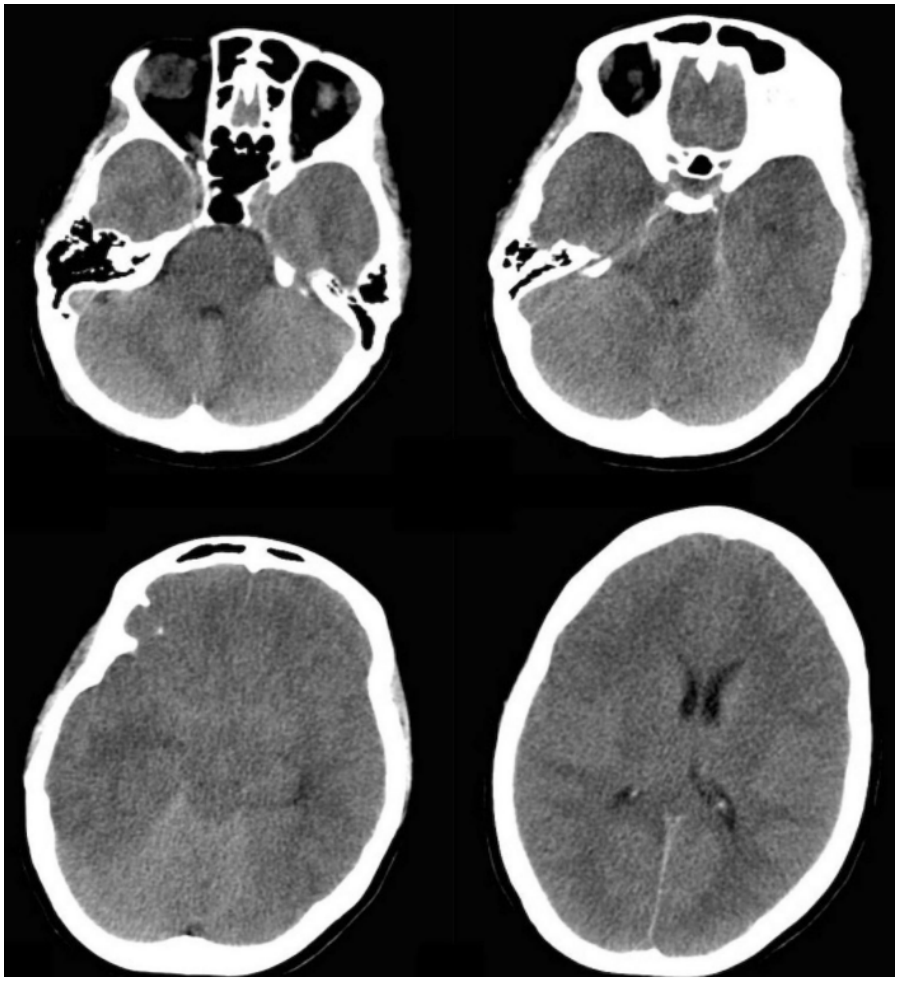

Head CT signs of diffuse cerebral edema. Axial non-contrast enhanced head computer tomography (CT) shows diffuse brain swelling predominantly involving infra-tentorial brain structures, associated with effacement of sulci and ventricles and decreased gray–white matter differentiation. The brainstem appears hypo-attenuated compared to other infra-tentorial brain structures

Qualitative EEG analysis

A total of 307 records belonging to the overall cohort (68 patients) have been visually assessed. Of them, 68 (22.1%) were recorded at baseline (pre-infusion) while 239 (77.9%) in the post-infusion period. The agreement between the two raters was strong (k=0.88). Figure 3 describes EEGs distribution among the cohort, considering the time of recording.

Figure 3. Flowchart of EEG records analyzed qualitatively and quantitatively

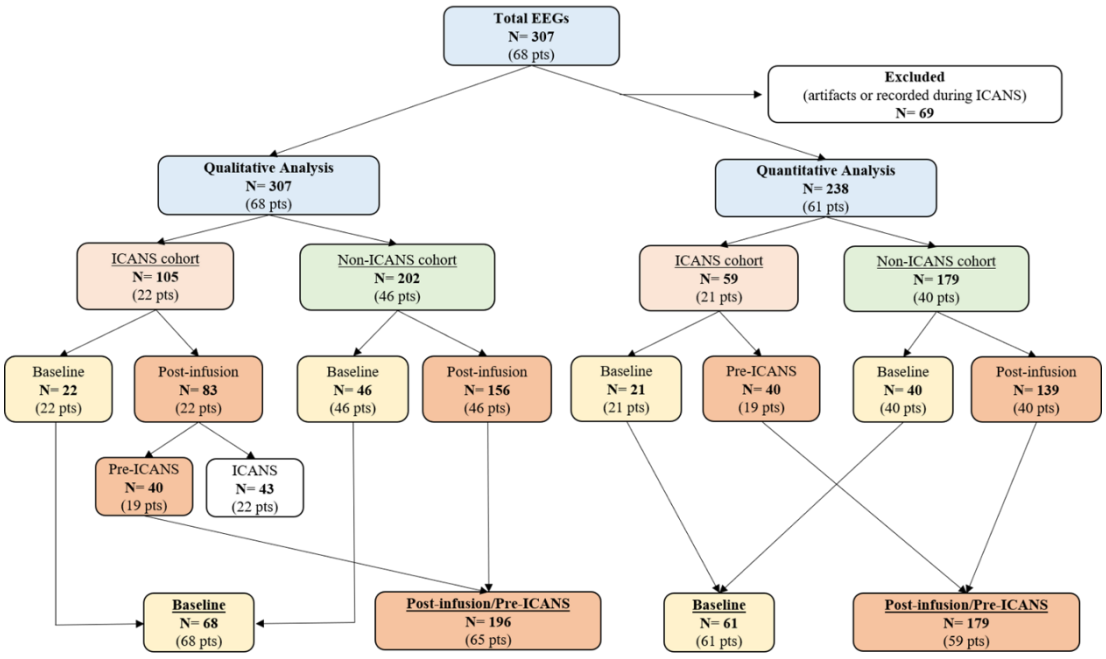

Baseline EEGs

Among baseline EEGs, 8/68 (11.8%) EEGs showed pathological findings. The grading score for these abnormalities resulted 1 (slightly abnormal) in 6/8 (75%) and 2 (moderately abnormal) in 2/8 (25%) cases. The specific features of the pathological EEGs at baseline are shown in Table 7.

Table 7. Features of the pathological baseline EEGs

Patient	PBF	Reactivity	Sporadic Theta	Sporadic Delta	State changes	EA	Significance	Score	ICANS
1.AA	Alpha	Present	++	+	-	-	Slightly abnormal	**1**	Yes
2.EB	Alpha	Present	++	+	Physio	-	Slightly abnormal	**1**	Yes
3.AB	Theta	Present	+++	++	-	-	Moderately abnormal	**2**	Yes
4.CD	Alpha	Present	-	-	Patho logical	-	Slightly abnormal	**1**	Yes
5.GI	Alpha	Present	-	-	Patho logical	-	Slightly abnormal	**1**	Yes
6.IM	Theta	Present	+++	++	-	-	Moderately abnormal	**2**	Yes
7.MM	Alpha	Present	-	-	Patho logical	-	Slightly abnormal	**1**	No
8.FR	Alpha	Present	++	+	-	-	Slightly abnormal	**1**	Yes

Post-infusion EEGs

Among the 239 EEGs recorded after the infusion day up to T14, 156 (65.3%) were from the non-ICANS cohort while 83 (34.7%) from the ICANS cohort. Regarding the latter, 40/83 (48.2%) EEGs were acquired before ICANS onset and eligible for comparative analysis with those of non-ICANS cohort.

The final pool of EEGs considered in the analysis included 196 records (156 non-ICANS and 40 pre-ICANS). Pathological findings were observed in 12/156 (7.7%) records of the non-ICANS cohort and in 20/40 (50%) pre-ICANS EEGs. Grading score resulted 1 (slightly abnormal) in 10 non-ICANS and 4 pre-ICANS, 2 (moderately abnormal) in 2 non-ICANS and 11 pre-ICANS, 3 (severely abnormal) in 5 pre-ICANS (while not observed in the non-ICANS cohort). Post-infusion EEG abnormalities anticipated ICANS onset by a median of 4 days (range: 1-9 days).

Examples of pathological EEGs gradings are given below:

Figure 4. Examples of the EEG grading

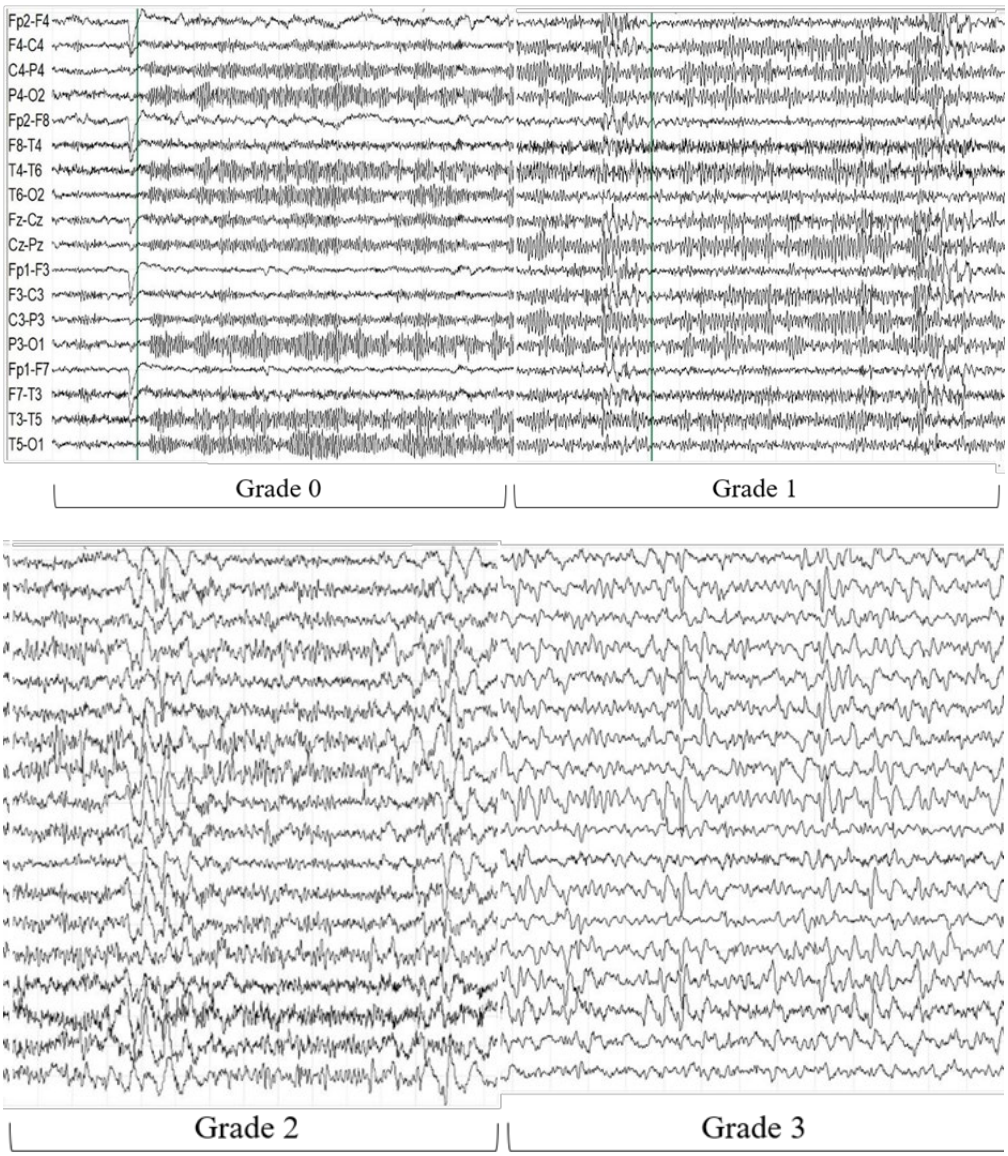

Legend:

Grade 0: normal EEG.

Grade 1: normal background (alpha rhythm) with sporadic diffuse theta activity at moderate prevalence.

Grade 2: predominant theta background frequency with sporadic diffuse delta activity at moderate prevalence.

Grade 3: predominant delta background frequency with anterior-predominant diffuse sharp waves at high prevalence

EEGs during ICANS

The EEG features in the 22 patients who experienced ICANS are summarized in the following table (CAVE: these have been excluded from the analysis).

Table 8. Features of the EEGs recorded during ICANS

EEG features	Patients (n)
Background slowing	22/22 (100%)
Non-epileptiform abnormalities	19/22 (86.4%)
Frontal intermittent delta activity	12/22 (54.5%)
Periodic discharges	1/22 (4.5%)
Epileptiform abnormalities	5/22 (22.7%)
Pathological state changes	12/22 (54.5%)

Risk of ICANS according to qualitative analysis

Risk of ICANS was significantly higher for both baseline EEGs showing grade 1 [HR 4.1; 95%CI 1.3-12.5] and grade 2 [HR 34.9; 95%CI 5.6-218.6] abnormalities (Table 2). Taken together, baseline EEGs abnormalities [HR 5.8; 95%CI 2.6-12.9] were corroborated as independent risk factor for ICANS in multivariable analysis [HR 3.3; 95%CI 1.3-8.7].

Table 9. Risk factors for ICANS: univariable and multivariable Cox regression models

Feature vs Reference Category	Unadjusted HR (95% CI)	p-value	Adjusted HR (95% CI)	p-value
Age	1.0 (0.9-1.0)	0.217		
Sex				
Male vs Female	4.0 (1.8-8.9)	**0.001**	3.7 (1.6-8.7)	**0.003**
Histology subtypes				
PMBCL vs DLBCL	4.7 (2.2-10.0)	**<0.001**		
MCL vs DLBCL	7.1 (3.5-14.2)	**<0.001**		
FL vs DLBCL	0.4 (0.0-3.0)	0.365		
Baseline EEG Abnormalities	5.6 (2.6-12.9)	**<0.001**	3.3 (1.3-8.7)	**0.014**
Ferritin				
>1000 vs <1000	2.0 (1.4-2.7)	**<0.001**	1.8 (1.3-2.6)	**0.001**
CAR T-cell Product				
Tisa-cell vs Axi-cell	0.4 (0.2-1.1)	0.074		
Brexu-cell vs Axi-cell	0.2 (0.3-1.4)	0.114		

Legend: HR = Hazard Ratio; 95% CI = 95% Confidence Interval

Post-infusion EEGs abnormalities were associated to a significant higher risk of ICANS when scored 2 [HR 11.6; 95% CI 4.4-30.5] and 3 [HR 9.7; 95% CI 2.6-36.6], while grade 1 abnormalities showed a trend of higher risk [HR 3.2; 95%CI 0.7-14.9].

Table 10. ICANS risk according to qualitative EEG: univariable Cox regression models

Baseline EEGs – fixed variable			
SCORE	**HR**	**[95% CI]**	**P-value**
0	Ref	-	-
1	4.1	1.3-12.5	**0.013**
2	34.9	5.6-218.6	**<0.001**
1+2	5.8	2.6-12.9	**<0.001**
Post-Infusion EEGs – time-dependent variable			
SCORE	**HR**	**[95% CI]**	**P-value**
0	Ref	-	-
1	3.2	0.7-14.9	0.139
2	11.6	4.4-30.5	**<0.001**
3	9.7	2.6-36.6	**<0.001**

Quantitative EEG analysis

From the total pool, 238/307 (77.5%) EEGs belonging to 61/68 patients (89.7%) were eligible for quantitative analysis (see Figure 3), while 69 EEGs were excluded due to artifacts (n= 58) or because not recorded in the pre-ICANS phase (n= 11).

No quantitative features at baseline were found to be significantly associated with a higher risk of ICANS development.

In post-infusion EEGs, energy values were significantly associated to the risk of ICANS development. Specifically, median theta energy [HR 1.10; 95%CI 1.03 - 1.16] and delta + theta/alfa ratio [HR 1.37; 95%CI 1.11-1.67] correlated to a higher risk of ICANS, while median beta energy emerged as protective factor [HR 0.91; 95%CI 0.85-0.97] (Table 11).

Table 11. ICANS risk in post-infusion EEGs according to quantitative analysis-Energy (median values) – univariable Cox regression models

Feature	HR	[95% CI]	p-value
Beta energy	0.91	0.85-0.97	**0.006**
Alpha energy	0.97	0.94-1.01	0.160
Theta energy	1.10	1.03 - 1.16	**0.001**
Delta energy	1.04	0.99-1.11	0.091
Delta+ theta/alfa ratio	1.37	1.11-1.67	**0.002**

Legend: HR = Hazard Ratio; 95% CI = 95% Confidence Interval

On the contrary, signal complexity and connectivity measures were not associated to a higher risk of ICANS development.

Cut-off values between tertiles were identified for theta energy and delta+ theta/alfa ratio. For both features, values above the cut-off between the second and the third tertile (2.2 and 0.31, respectively) were found to be significantly associated with a higher risk of developing ICANS (Table 12).

Table 12. Cut off values-Energy (time-dependent variables) in association of ICANS - univariable Cox regression models

Feature	HR	[95% CI]	P-value	Cut off
Theta energy				
First tertile	Ref	-	-	
Second tertile	0.4	0.7-2.2	0.282	*-0.56*
Third tertile	3.5	1.1-10.9	**0.029**	***2.2***
Delta + theta/alfa			-	
First tertile	Ref	-	0.406	*-0.16*
Second tertile	2.0	0.4-10.4	**0.068**	***0.31***
Third tertile	4.1	0.9-18.5		

Legend: HR = Hazard Ratio; 95% CI = 95% Confidence Interval

Differences in pre-infusion features between patients with and without baseline EEG abnormalities

Patients demonstrating abnormalities at baseline EEG were found to have significantly higher pre-infusion IL-6 (p=0.031) and CRP (p=0.014) serum levels. In contrast, demographics (age and sex), tumor-related factors (duration, disease status, stage, previous treatments), brain MRI abnormalities and neurological comorbidities did not differ among the two groups. Results of the post-hoc analysis are shown in Table 13.

Table 13. Differences in baseline features (pts with vs without EEG abnormalities)

	Baseline EEG abnormalities		**p-value**
	YES (n= 8)	**NO (n=60)**	
Age (years) (mean; range)	54.4 (19-68)	55.4 (21-70)	0.848
Female sex	4/8 (50%)	8/60 (13.3%)	0.174
Histology			
DLBCL	5/8 (62.5%)	45/60 (75%)	**0.017**
PMBCL	2/8 (25%)	6/60 (10%)	
MCL	0/8 (0%)	9/60 (15%)	
FL	1/8 (12.5%)	0/60 (0%)	
Bulky (>7cm)	4/8 (50%)	28/60 (46.7%)	0.859
Disease status			
Early refractory (<6 months)	7/8 (87.5%)	49/60 (81.7%)	0.413
Refractory (6-12 months)	1/8 (12.5%)	3/60 (5%)	
Relapsed (>12 months)	0/8 (0%)	8/60 (13.3%)	
Bridge therapy	7/8 (87.5%)	41/60 (68.3%)	0.054
Previous treatments (n) (mean, range)	2.5 (2-3)	3 (1-8)	0.487
ASCT	4/8 (50%)	19/60 (31.7%)	0.303
History of lymphoma (months) (mean, range)	19.6 (9-36)	55.3 (5-264)	0.826
Disease stage III-IV	7/8 (87.5%)	45/60 (75%)	0.434
RMN abnormalities	6/8 (75%)	34/60 (56.7%)	0.347
Pre-infusion serum inflammatory markers			
IL-6 (pg/mL)	36 (3.2-150)	14.5 (0.5-129)	**0.031**
IL-10 (pg/mL)	1.3 (0-4)	10.3 (0-185)	0.344
IL-8 (pg/mL)	38.3 (10-121)	45.9 (5-574)	0.956
Ferritin (ng/mL)	1473.4 (11-6787)	442 (11-6534)	0.202
CRP (mg/dL)	7.7 (0.1-19.2)	1.6 (0.1-18.5)	**0.014**
D-dimer (mg/L)	1.8 (0.19-7.32)	1.8 (0.2-6.3)	0.195

Discussion

In this large prospective cohort study, among 68 consecutive patients undergoing CAR-T therapy, one third developed ICANS, a percentage similar to that previously reported by other studies (Grant et al., 2022). ICANS was invariably associated with CRS, and all patients had progression of neurologic symptoms that occurred within a few hours to several days after onset, with a monophasic disease course. Death related to neurotoxicity occurred in two patients and was related to acute fulminant cerebral edema, a known and rare complications of neurotoxicity, although not described in details (Lee et al., 2019; Gust et al., 2020). As exemplified by our clinical vignette, the neurological deterioration may occur very rapidly. The pathophysiology of fulminant cerebral edema following CAR T-cell therapy remains not fully elucidated, yet histological and neuroimaging evidence supports cerebral vasogenic edema triggered cy cytokine-mediated BBB dysfunction as the underlying mechanism (Lee et al., 2019; Gust et al., 2020). Supporting cytokine-driven inflammation as the main putative mechanisms, there is a remarkable clinical-radiologic overlap between other neuro-inflammatory conditions among CySE, such as acute fulminant cerebral edema following viral infections (Krishnan et al., 2021). As the condition frequently has a fatal prognosis despite aggressive medical and surgical therapy, such as prompt administration of intravenous corticosteroids and craniotomy, new strategies to allocate pre-emptive therapies, even by means of novel effective anti-inflammatory treatments, are urgently warranted.

Clinical and EEG findings demonstrated a frontal predominant encephalopathy in the majority of patients. In our experience, a stereotypical subacute (hours to few days) progression of neurological manifestations may be depicted in patients who developed severe ICANS, characterized by early expressive aphasia and dysgraphia or paligraphia, frontal release signs, behavioral disinhibition, apathy, evolving in dysexecutive syndrome, akinetic mutism and eventually coma state. Paligraphia is another frequent feature strongly suggesting a frontal lobe dysfunction. Notably, the high prevalence of cognitive disturbances, especially dysexecutive syndrome and language impairment, has been recurrently observed in large real-life cohort studies (Rubin et al., 2019).

Regarding treatment, almost half of the patients who developed neurotoxicity were steroid-refractory and were administered second-line therapies such as anakinra and siltuximab. It is still not clear which is the optimal timing to use these agents, but the trend is to use them in earlier stages and even as prophylactic treatments. However, the impact on hematological outcomes of both steroids and anti-cytokines are yet to be defined.

EEG as a predictive biomarker of ICANS

The present study investigates the role of EEG in evaluating patients undergoing CAR-T therapy, positioning it as a valuable predictive biomarker of ICANS both prior to and following CAR T-cell infusion. We rigorously assessed a large dataset of EEG recordings from CAR T-cell therapy recipients, employing a protocol with predetermined evaluations for all subjects and blinded analysis by highly specialized experts. While interrater variability typically poses a problem in the interpretation of EEGs (Williams et al., 1985), the use of an ad-hoc rating scale designed to highlight gross differences allowed us to achieve strong agreement between raters. Additionally, for the first time to our knowledge, we applied quantitative signal analysis to EEGs in CAR-T therapy recipients.

Our findings underscore a dual role of EEG in assessing ICANS risk: firstly, by aiding in the identification of susceptible patients at baseline, and secondly, by predicting the clinical onset of ICANS after CAR T-cell infusion.

Patients with pre-infusion EEG abnormalities of any grade had a six times higher risk of developing ICANS compared to those with a normal EEG, a finding confirmed in the multivariable analysis with confounding factors, supporting preliminary findings obtained from an interim analysis of our cohort within this PhD project (Pensato et al., 2023) and the recent study from Hernani et al., 2024.

The precise significance of baseline EEG abnormalities is challenging to ascertain and requires to be investigated within the context of the pre-infusion period and intrinsic individual characteristics. Notably, no significant neurological comorbidities were present in our cohort. Instead, patients with baseline EEG abnormalities had higher serum IL-6 and CRP levels compared to those with normal EEG, in line with previous reports (Neelapu et al., 2018) suggesting that a pre-infusion inflammatory state may

predispose to the development of ICANS. In this respect, bridge therapies (i.e. chemotherapy and immunotherapy) may act exacerbating the hyperinflammatory condition (Edwardson et al., 2019). The pre-infusion inflammatory state may facilitate BBB damage, making the central nervous system more vulnerable to cytokine-mediated neuroinflammation secondary to CRS, which consistently anticipated ICANS in our cohort. Interestingly, pre-operative EEG abnormalities and elevated inflammatory markers may predict post-operative delirium (Capri et al., 2014; Bruzzone et al., 2023), a condition with a multifactorial pathogenesis that shares neuroinflammation with ICANS (Pensato et al., 2021). This could support the hypothesis that EEG abnormalities may reflect a non-specific marker of cerebral vulnerability and predisposition to cytokine storm-associated encephalopathies.

Visual evaluation proved to be highly effective in assessing the risk of ICANS at baseline outperforming quantitative analysis which, conversely, yielded non-significant results. Potentially contributing factors include the bias related to the selection of artifact-free segments in quantitative analysis, and the fact that most altered pre-infusion EEGs had sporadic slowing within a normal background activity, making the detection of abnormalities through quantitative analysis challenging. Thus, visual analysis of baseline EEG, which is available in all neurological centers involved in CAR-T therapy, could truly represent a crucial tool for screening candidates at risk of developing ICANS, also considering the increasing evidence of effective prophylactic protocols (Park et al., 2023; Strati et al., 2023).

Significantly reducing the incidence and severity of ICANS could have transformative implications. Currently, CAR T-cell therapy demands extensive resources, necessitating inpatient delivery and close outpatient monitoring due to the risk of severe toxicities, which may be mitigated by implementing a prophylactic strategy (Strati et al., 2023). The employment of EEG as predictive biomarkers for ICANS during the pre-infusion assessment could guide patient selection for randomized trials on prophylactic agents.

Our study also provides compelling evidence that abnormalities in post-infusional EEG can precede and potentially predict the clinical onset of ICANS. Although

ICANS is defined clinically, our findings suggest that neurotoxicity may manifest in the presymptomatic stage through EEG changes consistent with encephalopathy.

Both visual and quantitative assessments were able to detect EEG changes, with the former demonstrating superior performance. Nevertheless, quantitative analysis could prove beneficial in situations where continuous EEG monitoring is accessible, potentially allowing for automated detection of background slowing and subsequently triggering alerts for physicians.

These findings suggest that the incorporation of daily EEGs in neurological monitoring post-CAR T-cell infusion could facilitate early detection of ICANS onset.

Given the ease of application of EEG and the availability of effective therapies for ICANS, this protocol adjustment offers a significantly advantageous cost-to-benefit ratio. Indeed, even if ICANS is potentially fatal and characterized by a relevant morbidity, it can be controlled by immunomodulating treatments especially if promptly initiated (Park et al., 2023).

The EEG Grading Scale we have developed is easily applicable since the different grades are readily distinguishable based on the background activity's frequency band and the identification of gross EEG abnormalities. Nevertheless, it should be validated on a larger cohort of patients.

Study limitations

The monocentric design of the study constrains the generalizability of our findings. However, it concurrently streamlined coordination among researchers and yielded a homogeneous sample, thereby minimizing external confounding variables.

Furthermore, while the expertise of the evaluators and their blindness to clinical data ensure the accuracy of the assessments, it may also limit the generalizability of the findings to settings with less specialized resources or expertise, even though the grading scale we developed could be easily applicable even by neurologists with basic EEG training.

Conclusions

Our study establishes EEG as a pivotal tool for evaluating patients undergoing CAR T-cell therapy enhancing the ability to identify patients susceptible to ICANS who

could benefit from prophylactic treatment and, after the infusion, anticipating ICANS onset and allowing for timely interventions that are essential to improve patients' outcome. EEG emerges as an optimal predictive biomarker for ICANS owing to its widespread accessibility, simplicity of execution, prompt result acquisition, and distinctive ability to offer varied information beyond clinical assessment and laboratory investigations. Although further prospective studies are necessary to validate our findings, incorporating EEG monitoring into the clinical protocols for CAR T-cell therapy candidates and recipients already appears to be reasonable.

AIM 2: Neurological manifestations of COVID-19

Methods

Setting and population

A multicenter prospective cohort study design was applied. Consecutive patients admitted to three hospitals in the Emilia-Romagna region in Italy (S.Orsola-Malpighi and Maggiore Hospital in Bologna, Baggiovara Hospital in Modena) with PCR-proven COVID-19, were enrolled between March 2020 and April 2022.

Variables and index tests (S100B and NfL biomarkers)

Demographic, clinical and laboratory information were collected by the clinical team at the time of sample collection and reported in the medical records, which have been consulted for the obtainment of pertinent data for the present study.

Clinical data included: comorbidities, history of tabagism, precedent neurological disorders. Data about the detailed clinical course during hospitalization, including the modified Rankin score (mRS), were also recorded. In addition, COVID severity was considered, and defined based on the National Institute of Health guidelines (https://www.covid19treatmentguidelines.nih.gov/tables/therapeutic-management-of-hospitalized-adults/) into four classes: no need for oxygen therapy, low-flow oxygen therapy, high-flow oxygen therapy or non-invasive ventilation and mechanical ventilation (MV).

Laboratory information included: blood count, electrolytes, liver, renal and thyroid function tests, and inflammatory markers (i.e. fibrinogen, Il-6, PCR).

Serum samples were collected at a single time point in the acute or subacute phase after admission. The samples were aliquoted, labeled with pseudo-anonymized identifiers, and frozen immediately at −80°C. Analyses were performed at the Neurommunology lab of the OCB Modena Academic Hospital. S100B and NfL were assessed in serum samples and were used as index test in the diagnostic analysis.

Reference standard: neuro-COVID diagnosis

Patients with a newly diagnosed neurological disorder of any type, developed during the prodromal, acute respiratory, or recovery phase of COVID-19 infection during

hospitalization, were considered eligible. Patients were enrolled in the study solely after a comprehensive evaluation by neurology specialists. Neurological consultations were conducted in the neurology departments, stroke units, Neuro-COVID wards, and neuro-ICUs. Whenever neuro-COVID symptoms were confirmed, the patient was offered the opportunity to participate in the study and classified as neuro-COVID, in contrast to the "control" group of patients without neurological manifestations (COVID-w/o Neuro). Neuro-COVID patients were further classified as follows: extra-cranial neuro-COVID (e.g., neuropathies, radicoloneuritis, myelitis), mild encephalopathy (e.g., confusion, agitation, ideomotor slowing, epileptic seizure) and severe encephalopathy (e.g., delirium, status epilepticus, coma).

Prognostic analysis

The outcome for the prognostic evaluation was the difference between mRS at discharge and mRS at hospital admission: at least one-unit increase indicated the worsening of the disease. The association with the outcome was evaluated for demographic, clinical and laboratory variables.

Statistical analysis

Continuous descriptive variables were presented using median and interquartile range (IQR). The Shapiro-Wilk test was used to evaluate the normal data distribution. Categorical variables were presented using absolute numbers (n) and percentages (%). Two-group comparisons were assessed using Mann-Whitney U-test for continuous variables and with the Chi-square test for categorical variables.

In the diagnostic analysis receiver operating characteristic (ROC) analyses with relative 95% Confidence Intervals (95% CI) were performed to evaluate the diagnostic accuracy of NfL and S100B biomarkers between Neuro-COVID and COVID patients without neurological symptoms (COVID-w/o Neuro).

Spearman's Rho correlation for continuous variables, and Mann-Whitney U-test for categorical variables, were used to evaluate the variables associated with the two biomarkers. The results were presented with Rho coefficients.

In the cross sectional analysis (time of sample collection) univariable and multivariable linear regression models were used to evaluate the association between

variables and biomarkers (dependent variables). The biomarker levels were not normally distributed and were transformed into natural logarithms. The results were presented with Beta coefficients (β) and 95% CI.

In the prognostic analysis univariable and multivariable logistic regression models were used to evaluate the association between the variables and worsening of disease (at least one-unit increase of mRs scale from hospital admission to discharge - dependent variable). The results were presented with Odds Ratio (OR) and 95% CI.

Statistical analyses were performed using Stata v. 16.1

Standard protocol approvals

The study was approved by the institutional review board Ethical Committee AVEC (protocol number: 925-2021-OSS-AUSLBO-21182). Written informed consent was obtained from either enrolled patients or from their legal representatives, both for study participation and data publication.

Results

A total of 279 patients (153 males, median age 76.7 years) were included in the analysis. Demographic, clinical, and laboratory data for the total sample, as well as for the COVID-w/o Neuro and Neuro-COVID groups, are presented in Table 14. Serum NfL levels were assessed in 276 patients, whereas serum S100B was measured in 268 patients. The median time from admission to sample collection was 3 days.

According to COVID severity, 119 patients (42.7%) did not require oxygen therapy, 108 (38.7%) required low-flow oxygen therapy, 40 (14.3%) required high-flow oxygen therapy or non-invasive ventilation and 12 required mechanical ventilation (Table 14).

Sixty-nine (24.7%) patients developed Neuro-COVID and were grouped as follows: 9 (13.0%) had extra-cranial neuro-COVID, 36 (52.2%) had mild encephalopathy and 24 (34.8%) had severe encephalopathy (Table 14).

Table 14. Characterization of the COVID-19 study cohort

	Total sample N = 279	COVID-w/o Neuro N = 210	Neuro-COVID N = 69	p
Age				
Median (IQR)	76.7 (59.8-84.4)	77.5 (63.4-84.4)	72.4 (58.2-85)	0.391
Sex, N (%)				
M	153 (54.8)	107 (51)	46 (66.7)	**0.023**
COVID-19 severity (NIH), N (%)				
No oxygen therapy (OT)	119 (42.7)	88 (41.9)	31 (44.9)	
Low-flow OT	108 (38.7)	84 (40)	24 (34.8)	
High-glow OT	40 (14.3)	30 (14.3)	10 (14.5)	0.765
Mechanical Ventilation	12 (4.3)	8 (3.8)	4 (5.8)	
NeuroCOVID classification, N (%)				
Extra-cranial neuro-COVID			9 (13)	
Mild encephalopathy			36 (52.2)	<0.001
Severe encephalopathy			24 (34.8)	
Previous neurological disorders, N (%)				
Yes	100 (35.8)	64 (30.5)	36 (52.2)	**0.001**
Pulmonary disease, N (%)				
Yes	57 (20.4)	44 (23)	13 (18.8)	0.706
Smoke, N (%)				
Yes	66 (23.7)	34 (18.8)	9 (15)	0.261
Obesity, N (%)				
Yes	51 (18.3)	42 (20)	9 (13)	0.195
DM, N (%) (Diabetes mellitus)				
Yes	82 (29.4)	62 (29.5)	20 (29)	0.932
Ischemic heart disease , N (%)				
Yes	51 (18.3)	42 (20)	9 (13)	0.195
Ipertension, N (%)				
Yes	187 (67)	139 (66.2)	48 (69.6)	0.605
CKD, N (%) (Chronic kidney disease)				
Yes	62 (22.2)	48 (22.9)	14 (20.3)	0.656
Immunosuppression, N (%)				
Yes	29 (10.4)	27 (12.9)	2 (2.9)	**0.021**
Fever, N (%)				
Yes	53 (19)	41 (19.5)	12 (17.4)	0.695
Amines, N (%)				
Yes	4 (1.4)	2 (1)	2 (2.9)	0.256
Steroids, N (%)				
Yes	114 (40.9)	94 (44.8)	20 (29)	**0.021**
Tocilizumab, N (%)				
Yes	2 (0.7)	2 (1)	0 (0)	0.608
sNFL				
Median (IQR)	72.7 (35.5-175.5)	68.3 (34.3-153)	110 (44.6-244)	
missing	1	0	1	**0.035**
S100B serum				
Median (IQR)	12 (10.1-13.2)	0.13 (0.08-0.23)	0.11 (0.08-0.23)	
missing	11	1	10	0.573
S100B liquor				
Median (IQR)	2.3 (1.8-3.3)	-	2.3 (1.8-3.3)	
missing	42		42	-

Q/S100 Median (IQR) missing	0.05 (0.03-1) 43	-	0.05 (0.03-1) 43	-
K-index Median (IQR) missing	1.6 (1.2-3.4) 48	-	1.6 (1.2-3.4) 48	-
Time symptoms-sampling Median (IQR)	3 (1-11)	3 (1-12)	2 (1-6)	0.014
White Blood Cells Median (IQR) missing	6.6 (4.3-9.3) 1	5.9 (4-8.9) 0	7.3 (5.5-10.2) 1	**0.007**
Lymphocytes Median (IQR) missing	1 (0.7-1.5) 27	1 (0.7-1.4) 22	1 (0.8-1.6) 5	0.282
Platelets Median (IQR) missing	216.5 (166-281) 1	215.5 (166-280) 0	227.5 (164.5-295.3) 1	0.692
Haemoglobin Median (IQR) missing	4.1 (1.1-10.1) 1	11.9 (10-13) 0	12.5 (10.4-13.7) 1	0.129
Na (sodium) Median (IQR) missing	139 (136-141) 6	139 (136-141) 3	140 (137-144) 3	0.006
K (potassium) Median (IQR) missing	4 (3.7-4.4) 8	4 (3.7-4.4) 5	4.1 (3.7-4.4) 3	0.799
PCR Median (IQR) missing	4.1 (1.1-10.1) 14	4.9 (1.4-11.5) 11	1.9 (0.5-6.1) 3	**<0.001**
LDH Median (IQR) missing	0.9 (0.7-1.4) 139	235.5 (194-338) 108	276.5 (204-386) 31	0.171
AST Median (IQR) missing	25 (18-37) 23	24 (18-36) 17	30 (17-45) 6	0.242
Total bilirubin Median (IQR) missing	0.7 (0.5-0.9) 53	0.6 (0.5-0.9) 40	0.7 (0.5-0.9) 13	0.528
CPK Median (IQR) missing	75 (34-177) 108	66 (31-146) 94	101 (49-262) 14	**0.009**
Creatinine Median (IQR) missing	3.2 (0.9-535) 10	0.9 (0.7-1.5) 7	1 (0.7-1.4) 3	0.976
PT (prothrombin time) Median (IQR) missing	1.14 (1.08-1.29) 42	1.14 (1.08-1.3) 32	1.13 (1.08-1.25) 10	0.392
ApTT (activated partial thromboplastin time) Median (IQR) missing	1.1 (1-1.4) 54	1.2 (1-1.5) 41	1 (0.9-1.1) 13	<0.001
D-dimer Median (IQR) missing	21 (9.8-48.8) 204	1.1 (0.8-3.1) 164	1,118 (477-1,690) 40	**<0.001**
Fibrinogen Median (IQR) missing	476 (385-579) 148	485 (412-600) 123	434.5 (346) 25	0.014

Ferritin Median (IQR) missing	260 (91-506) 177	266.5 (95-542) 124	177 (59.5-349) 53	0.279
IL-6 Median (IQR) missing	2 (0-3) 162	21.3 (9.8-48.8) 120	19.4 (9.8-43.8) 42	0.836
mRs (modified ranking scale) before admission Median (IQR)	1 (0-2)	1 (0-2)	1 (0-2)	0.762
mRs discharge Median (IQR) missing	18 (6.5) 3	1 (0-3) 1	3 (1-4) 2	**<0.001**
Duration of admission Median (IQR) missing	13 (7-25) 6	13 (7-24) 4	16 (7-38) 2	0.142
Deceased during hospitalization, N (%) Yes	18 (6.5)	11 (5.2)	7 (10.3)	0.141

Clinical features

In the Neuro-COVID group compared to COVID-w/o Neuro there was a significantly larger proportion of men [46 (66.7%) vs 107 (51%); p = 0.023], presence of previous neurological disorders [36 (52.2%) vs 64 (30.5%); p = 0.001], and higher mRS at discharge [median values 3 vs 1; p < 0.001]; moreover, the Neuro-COVID group presented with a lower proportion of patients with immunosoppression[2 (2.9%) vs 27 (12.9%); p = 0.021] and receiving steroids [20 (29%) vs 94 (44.8%); p = 0.021] (Table 14).

Laboratory features

In the Neuro-COVID group compared to COVID-w/o Neuro, there were significantly higher values of NfL [median values 110 vs 68.3 pg/mL; p = 0.035], white blood cells [median values 7.3 vs 5.9 10^9/L; p = 0.007], serum sodium [median values 140 vs 139 mmol/L; p = 0.006], CPK [median values 101 vs 66 U/L; p = 0.009], and D-dimer [median values 1.118 vs 1.1 mg/L; p < 0.001], whereas the following were lower: CRP [median values 1.9 vs 4.9 mg/dL; p < 0.001], aPTT [median values 1 vs 1.2; p < 0.001], and fibrinogen [median values 434.5 vs 485 mg/dL; p = 0.014] (Table 14).

Diagnostic analysis – S100B and NfL biomarkers

The ROC analysis showed very low accuracy in the discrimination between Neuro-COVID group vs. COVID-w/o Neuro group for both NfL and S100B, with an area under the curve (AUC) values respectively of 0.58 (95% CI = 0.51-0.66) and 0.48 (95% CI = 0.39-0.56).

Cross-sectional analysis

Associations between S100B, NfL and the clinical factors are reported in Table 15.

Table 15. Associations between NfL, S100B, and other clinical variables

	NFL	p	S100B	p
Age				
Rho coefficient	0.296	**<0.001**	0.250	<0.001
Sex, N (%)				
M	74.6 (35.9-225)		0.11 (0.07-0.21)	
F	68.3 (34.9-153)	0.233	0.15 (0.09-0.32)	0.004
Previous neurological disorderS, N (%)				
Yes	78 (44-240)		0.14 (0.09-0.26)	
No	69.7 (33.1-164)	**0.049**	0.13 (0.07-0.23)	0.099
Pulmonary disease, N (%)				
Yes	85.3 (54-153)		0.15 (0.10-0.29)	
No	68.7 (32.7-180)	0.063	0.11 (0.08-0.22)	0.032
Smoke, N (%)				
Yes	69.1 (37.3-176)		0.13 (0.08-0.21)	
No	72.7 (33.4-177.5)	**0.019**	0.13 (0.08-0.26)	0.476
DM, N (%) (Diabetes mellitus)				
Yes	109.5 (44-240)		0.13 (0.09-0.23)	
No	68.5 (32.1-153)	**0.004**	0.13 (0.08-0.23)	0.461
Ischemic heart disease , N (%)				
Yes	116 (56.7-251)		0.13 (0.09-0.25)	
No	67.8 (32.5-171)	**0.001**	0.13 (0.08-0.23)	0.810
Ipertension, N (%)				
Yes	77.3 (45.7-205)		0.13 (0.08-0.26)	
No	42.5 (12.3-106)	**<0.001**	0.11 (0.06-0.20)	0.042
CKD, N (%) (Chronic kidney disease)				
Yes	149 (73.9-354)	**<0.001**	0.16 (0.10-0.28)	0.025
No	61.4 (29.8-124)		0.13 (0.08-0.22)	
Haemoglobin				
Rho coefficient	-0.509	**<0.001**	-0.168	0.006
PCR				
Rho coefficient	0.110	0.076	0.192	0.002
Creatinine				
Rho coefficient	0.343	**<0.001**	0.183	0.003
mRs before admission				
Rho coefficient	0.362	**<0.001**	0.210	<0.001
NeuroCOVID category, N (%)				
No neurological symptoms	68.3 (34.3 – 153)		0.128 (0.078 – 0.229)	
Extra-cranial neuro-COVID	128 (60.0 – 225.0)		0.101 (0.041 – 0.182)	
Mild encephalopathy	78.4 (34.8 – 187.5)		0.106 (0.075 – 0.181)	
Severe encephalopathy	119 (73.6 – 416)	**0.030**	0.155 (0.084 – 0.326)	0.597
COVID-19 severity (NIH), N (%)	53.8 (27.2-150)		0.11 (0.07-0.21)	
No oxygen therapy (OT)	81.8 (43.4-192)		013 (0.08-0.29)	
Low-flow OT	66.4 (37.9-139.5)		0.13 (0.10-0.32)	
High-flow OT	117 (91.4-274.5)	**0.005**	0.14 (0.08-0.23)	0.076
Mechanical Ventilation				

* Median sNFL value (IQR) for categorical variables or Spearman correlation for continuous variable.

After multivariable regression models the clinical factors positively associated with NfL were age (β = 0.02, 95% CI = 0.01-0.03; p = 0.001), Chronic Kidney disease (CKD) (β = 0.68, 95% CI = 0.34-1.01; p < 0.001), extracranial disease vs COVID-w/o Neuro (β = 0.76, 95% CI = 0.12-1.4; p = 0.021), severe encephalopathy vs COVID-w/o Neuro (β = 0.56, 95% CI = 0.13-0.99; p = 0.011), low-flow oxygen therapy vs no O_2 therapy (β = 0.32, 95% CI = 0.02-0.61; p = 0.034), MV vs no O_2 therapy (β = 0.80, 95% CI = 0.19-1.4; p = 0.011). The clinical factors found to be inversely associated with NfL were CRP (β = -0.03, 95% CI = -0.05/-0.01; p = 0.006) and hemoglobin (β = -0.22, 95% CI = -0.28/-0.15; p < 0.001).

The clinical factor found to be positively associated with S100B was age (β = 0.01, 95% CI = 0.01-0.02; p = 0.001), while the clinical factor found to be inversely associated with S100B was Hb (β = -0.06, 95% CI = -0.11/-0.004; p = 0.037).

Prognostic analysis

Associations between worsening and not-worsening and the clinical features and biomarkers levels are reported in Table 16.

Table 16. Characteristics of the study cohort by type of worsening

	Nor worsening N = 192	**Worsening N = 84**	**p**
Age			
Median (IQR)	76 (60-84.5)	78 (62.1-84.3)	0.752
Sex, N (%)			
M	108 (71.1)	44 (28.9)	0.552
NeuroCOVID classification, N (%)			
No neurological symptoms	160 (83.3)	49 (58.3)	<0.001
Extra-cranial neuro-COVID	1 (0.5)	7 (8.3)	
Mild encephalopathy	23 (12)	13 (15.5)	
Severe encephalopathy	8 (4.2)	15 (17.9)	
COVID-19 severity (NIH), N (%)			
No oxygen therapy (OT)	90 (46.9)	28 (33.3)	0.001
Low-flow OT	74 (38.5)	33 (39.3)	
High-flow OT	26 (13.5)	14 (16.7)	
Mechanical Ventilation (MV)	2 (1)	9 (10.7)	
Previous neurological disorders, N (%)			
Yes	75 (39.1)	24 (28.6)	0.095
Pulmonary disease, N (%)			
Yes	39 (20.3)	18 (21.4)	0.833
Smoke, N (%)			
Yes	52 (31.5)	14 (19.2)	0.050
Obesity, N (%)			
Yes	36 (18.8)	14 (16.7)	0.679

DM, N (%) **(Diabetes mellitus)** Yes	59 (30.7)	23 (27.4)	0.575
Ischemic heart disease , N (%) Yes	39 (20.3)	12 (14.3)	0.235
Ipertension, N (%) Yes	127 (66.2)	59 (70.2)	0.505
CKD, N (%) **(Chronic kidney disease)** Yes	46 (24)	15 (17.9)	0.261
Immunosuppression, N (%) Yes	23 (12)	6 (7.1)	0.228
Fever, N (%) Yes	37 (19.3)	15 (17.9)	0.782
Amines, N (%) Yes	1 (0.5)	3 (3.6)	0.085
Steroids, N (%) Yes	81 (42.2)	32 (38.1)	0.525
Tocilizumab, N (%) Yes	2 (1)	0 (0)	0.206
sNFL Median (IQR)	65.2 (33.5-138)	110 (47.4-270)	**0.002**
S100B liquor Median (IQR)	1.9 (1.7-2.1)	2.5 (1.8-3.5)	0.100
S100B serum Median (IQR)	0.12 (0.08-0.20)	0.15 (0.09-0.34)	0.019
QS100 Median (IQR)	0.03 (0.03-0.07)	0.06 (0.03-0.1)	0.617
K-index Median (IQR)	1.8 (1.2-3.4)	1.6 (1-2.9)	0.760
Time symptoms-sampling (days) Median (IQR)	3 (1-11)	4 (1-8)	0.851
White Blood Cells Median (IQR)	5.8 (4-8.8)	7.8 (5.3-10.7)	0.002
Lymphocytes Median (IQR)	1 (0.7-1.4)	1.1 (0.7-1.6)	0.392
Platelets Median (IQR)	216 (163-281)	221 (171.5-280)	0.999
Haemoglobin Median (IQR)	12.1 (10.1-13.2)	11.9 (9.9-13.2)	0.461
Na Median (IQR)	139 (136-141)	139 (136-141.5)	0.800
K Median (IQR)	4 (3.7-4.4)	4.1 (3.6-4.5)	0.918
PCR Median (IQR)	4.1 (1.2-9.8)	4.3 (0.8-10.2)	0.758
LDH Median (IQR)	232 (185-326)	298 (224-439)	0.003
AST Median (IQR)	24 (17-36)	29 (18-37)	0.173
Total bilirubin Median (IQR)	0.7 (0.5-0.9)	0.7 (0.5-0.9)	0.486
CPK Median (IQR)	71.5 (30.5-154)	71.5 (30.5-154)	0.666
Creatinine Median (IQR)	0.9 (0.7-1.4)	0.9 (0.7-1.4)	0.548

PT Median (IQR)	1.1 (1.1-1.3)	1.1 (1.1-1.3)	0.692
apTT Median (IQR)	1.2 (1-1.5)	1.1 (1-1.3)	0.031
D-dimer Median (IQR)	1.1 (0.7-23.6)	17.7 (1.7-1,351)	<0.001
Fibrinogen Median (IQR)	473 (411-569)	486 (345.5-599)	0.835
Ferritin Median (IQR)	194 (86-496)	268 (190-542)	0.188
IL-6 Median (IQR)	20.4 (6.6-48.8)	22.9 (16.2-43.8)	0.103
mRs before admission Median (IQR)	1 (0-3)	1 (0-2)	0.423
mRs discharge Median (IQR)	1 (0-3)	3 (2-4.5)	<0.001
Duration of admission Median (IQR)	34.3 (37.1)	22 (12-46)	<0.001
Deceased during hospitalization, N (%) Yes	0 (0)	18 (21.4)	<0.001

After multivariable regression models the variables that contributed to worsening of mRS were MV vs no O_2 therapy (OR= 9.56, 95% CI = 1.67-54.75; p = 0.011), severe encephalopathy vs COVID-w/o Neuro (OR = 5.10, 95% CI = 1.58-16.19; p = 0.006), S100B (OR = 2.62, 95% CI = 1.10-6.46; p = 0.037) and duration of admission(OR = 1.03, 95% CI = 1.01-1.05; p = 0.001). Predictors of worsening after multivariable regression analysis are reported in Table 17.

Table 17. Predictors of clinical worsening after multivariable logistic regression

Variables	Odds Ratio	95% CI	p-value
COVID-19 severity (NIH), N (%) No oxygen therapy (OT) vs.			
Low-flow OT	1.21	0.59 – 2.48	0.611
High-flow OT	1.33	0.52 – 3.39	0.547
Mechanical Ventilation	**9.55**	**1.67 – 54.75**	**0.011**
NeuroCOVID classification, N (%) No neurological symptoms vs.			
Extra-cranial neuro-COVID	10.16	0.89 – 115.92	0.062
Mild encephalopathy	1.91	0.77 – 4.70	0.159
Severe encephalopathy	**5.06**	**1.58 – 16.19**	**0.006**
sNFL	0.999	0.999 – 1.002	0.753
S100B_serum	**2.62**	**1.06 – 6.46**	**0.037**
Duration of admission	**1.03**	**1.01 – 1.05**	**0.001**
mRs before admission	0.84	0.66 – 1.09	0.195

Discussion

In this study involving a large cohort of COVID-19 patients, serum NfL and S100B biomarkers were not accurate in discriminating cases with neurological manifestations from those without. However, S100B displayed a prognostic value, as the elevated levels of this biomarker predicted in our cohort a functional worsening. Besides, our results are in agreement with findings of no utility of S100B in determining COVID-19 acute severity, meant as necessity of respiratory support according to NIH classification (Sahin et al., 2022).

Nonetheless, NfL displayed a positive correlation with severe encephalopathy and extracranial neurological manifestations, compared to the population which did not develop any neurological symptoms. No direct relation was observed in patients with mild encephalopathy. These findings suggest that NfL might be less sensitive for mild conditions, and that finding a high level of NfL in patients with COVID-19 should be considered as a potential biomarker of severe neurological involvement and the need for tempestive treatment. The fact the NfL might not be able to effectively discriminate neuro-COVID patients might stem from the presence of neuroaxonal injury also in mild COVID-19 patients and those without neurological manifestations (Abdelhak et al., 2023).

The prediction of neurological complications is a fundamental tool in the management of patients with high-severity COVID-19, as it has been observed that the development of CNS involvement can severely impact patient outcome (Guerrero et al., 2021). In particular, patients admitted to the hospital with only respiratory symptoms but who developed neurological conditions during the hospitalization are reported to progress more frequently with a more severe course, with increased intubation and mechanical ventilation requirements, although it is more frequent in patients presenting with more compromised respiratory function (Gusap et al., 2022). Accordingly, in addition to S100B, the functional prognosis in our cohort was impacted by the occurrence of MV and the presence of severe encephalopathy.

Our results are also in agreement with early pandemic findings of the prognostic role of elevated D-dimer levels, especially when higher than 1 μg/mL, in patients with poor outcome (Zhou et al., 2020). D-dimer is a marker of increased coagulation activity,

determined by a systemic pro-inflammatory cytokine response, which can contribute to plaque disrupture predisposing to ischemia and thrombosis. Also, the presence of ACE2, the receptor for SARS-CoV-2, in the vascular endothelial cells, can contribute to the mechanism (Zhou et al., 2020).

The mechanisms underlining the central and peripheral nervous system involvement during the infection are still not clearly defined, although it is evident that multi-factorial damage of the BBB can occur and explain the clinical manifestations. In particular, it has been shown that SARS-CoV-2 may determine a state of hypercoagulability and hyperinflammation that may lead to the disruption of the BBB, also by interacting with the ACE2 receptors in the capillary walls of the brain circulation (Baig et al., 2020).

The possible role in the onset of neurological symptoms of systemic inflammation and The possible role in the onset of neurological symptoms of systemic inflammation and BBB disruption has been investigated through the correlation of blood biomarkers of BBB disruption, neuronal damage (NfL), and systemic inflammation and clinical findings (Baig et al., 2020). Specifically, it has been observed that blood biomarkers of BBB disruption and neuronal damage are high in COVID-19 patients, with levels similar to or higher than in patients with other neurological illnesses (i.e. ALS) (Bonetto et al., 2022). Higher levels of NfL in patients with severe COVID and neurological manifestations were previously observed and are in line with our findings (Bonetto et al., 2022).

Additionally, we found that neuro-COVID was negatively correlated with immunosuppression and steroid usage is noteworthy and could be interpreted in various ways. On one hand, reduced steroid therapy might have resulted in decreased neuroprotection, subsequently leading to the development of neurological symptoms. On the other hand, neuro-COVID patients may have required less intensive systemic treatment. Nevertheless, the severity of acute respiratory COVID-19 was similar between the two groups.

We have also observed a relation between high levels of both NfL and S100B and low hemoglobin, which we considered as a sign of systemic inflammation, as hemoglobin tends to drop in the presence of activation of the inflammatory system.

The impact of our research is that we caution other researchers not to overinterpred results obtained in critical ill patients displaying several features affecting the fate of these biomarkers. Notably, we found high levels of the biomarkers in patients with reduced or absent neurological manifestations, suggesting potential confounding factors such as reduced kidney filtration impacting biomarker levels.

The study presents some limitations which may have influenced the investigated associations. First, the control group (i.e., non-neuro-COVID) was not visited by a neurologist, determining a possibile underestimation of neurological symptoms in our cohort. Especially for patients with severe disease, it is possible that concomitant nervous damage was present and not captured, acting as a confounder impacting the specificity of both biomarkers. Secondarily, not all data were available for the entire population, potentially leading to an overestimation or underestimation of the relevance of some parameters. Additionally, the mRS was used for the prognostic analysis, although this disability score is designed for neurological conditions and is usually evaluated at follow-up evaluations, not included in the study design due to healthcare challenges during the pandemic. As no gold-standard classification of neuro-COVID symptoms exists, we classified them arbitrarily into three categories: although these may not capture perfectly the whole spectrum of neurological manifestations, these allow the discrimination between milder and more severe cases. Finally, there was not a strict timing in sampling, therefore some values may have been sampled at different stages of their evolutionary trend.

Conclusions

We found that blood S100B nor NfL biomarkers were able to discriminate between patients with and without neurological manifestations.. While S100B was not associated with neuro-COVID, in alignment with previous findings, it showed prognostic value by predicting poor outcomes in COVID patients. On the other hand, serum NfL was associated with extracranial neurological manifestations and severe encephalopathy, corroborating its potential as a biomarker of severe neurological conditions. Our study raises important considerations regarding the interpretation of biomarker results in critically ill patients with multiple comorbidities. We suggest caution against overinterpreting biomarker data in these complex conditions,

emphasizing the need to account for factors such as renal function and systemic inflammation.

AIM 3: FIRES

Methods

Population and setting

In this monocentric, prospective, study, we included all consecutive adult patients with with FIRES admitted to IRCCS Istituto delle Scienze Neurologiche – Azienda USL di Bologna, from January 2020 to December 2023. FIRES diagnosis was established based on the international consensus definition (Hirsch et al., 2018).

Procedures and data collection

All patients underwent the diagnostic procedures detailed in Wickstrom et al., 2022:

- Blood and serum: complete blood count, electrolytes, liver and renal function, CRP, standardized cell-based assay (CBA) kit (Euroimmun) for detecting antibodies against neuronal surface antigens (LGI1, CASPR2, NMDAR, AMPAR, GABABR, and DPPX), MOG, GAD65, anti-thyroid, paraneoplastic, SLE panel, ANA, ANCA, cytokines, immunoglobulins, viral serology (HIV, HSV, SARS-CoV-2), bacterial serology, blood cultures for bacteria and fungi.
- CSF: cells (count and cytology), protein, glucose, lactate, IgG/albumin ratio, immunoelectrofocusing, cytokines when available, PCR for common viral and bacterial causes of meningoencephalitis, onconeural antibodies, a standardized CBA kit (Euroimmun) for detecting antibodies against neuronal surface antigens (LGI1, CASPR2, NMDAR, AMPAR, GABABR, and DPPX) in addition to tissue-based approaches (IFI on rat brain).
- Continuous EEG
- Brain MRI with gadolinium contrast
- Computed tomography of the thorax and abdomen
- Toxicology screen

Data on treatment interventions (antiseizure medications, anesthetics, immunotherapies) and patient outcomes were also collected (duration of SE, duration of ICU stay, outcome calculated with mRS).

Ethics

Informed written consent was obtained from all patients for participation in the study.

Results

Four patients (three males) with a mean age of 24 years (range: 18-40 years) and no significant past medical history presented with FIRES. The main features are summarized in Table 18.

Table 18. Characteristics of the FIRES cohort

	Case 1	**Case 2**	**Case 3**	**Case 4**
Age at onset, sex	20 yo, male	40 yo, female	18 yo, male	19 yo, male
Ethnicity	Caucasian	Caucasian	Asian	Caucasian
Follow-up	33 months	47 months	11 months	30 months
Antiseizure medications	10 (LEV, LAC, PHT, PER, BRV, PB, ZNS, VPA, CBD, CLB)	10 (LEV, LAC, PHT, PER, BRV, PB, ZNS, VPA, TPM, CLB)	9 (LEV, LAC, PHT, PER, BRV, PB, VPA, CBD, CLB)	8 (LEV, LAC, PHT, PER, BRV, PB, VPA, TPM)
Anesthetics	PRO, MDZ, KET	PRO, MDZ, KET, TPS	PRO, MDZ, KET	PRO, MDZ, KET
Immunotherapies	MP, PLEX, IVIg, anakinra	MP, IVIg, RTX	MP, IVIg, CP	MP, PLEX, IVIg, CP
Other therapies for SE	VNS, KD	None	VNS	None
SE duration	90 days	45 days	34 days	59 days
ICU stay	111 days	87 days	84 days	69 days
Relapse	Yes, at 12 months	No	No	Yes, at 12 months
Outcome (mRS)	2	2	4	2

Abbreviations: BRV, brivaracetam; CBD, cannabidiol; CLB, clobazam; CNZ, clonazepam; CP, cyclophosphamide; IVIg, intravenous immunoglobulin; KD, ketogenic diet; KET, ketamine; LAC, lacosamide; LEV, levetiracetam; MP, methylprednisolone; mRS, modified Rankin Scale; PB, phenobarbital; PER, perampanel; PHT, phenytoin; PRO, propofol; RTX, rituximab; SE, status epilepticus; TPM, topiramate; TPS, sodium tiopenthal; VNS, vagus nerve stimulation; ZNS, zonisamide

Fever preceded the onset of SE by an average of 5 days (range: 3-6 days). All cases exhibited generalized convulsive SE after an average of 5 days of febrile illness .

Etiology was cryptogenic despite an extensive diagnostic work-up, including the examinations detailed in the methods for all patients..

Brain MRI in the acute stage showed a combination of T2-hyperintentisities and swelling in the following regions: claustrum (n=3) (example in Figure 5), mesial temporal lobe (n=2), cingulate cortex (n=2), pulvinar (n=2), frontal lobe (n=1).

Figure 5. Brain MRI in case 2: the claustrum sign

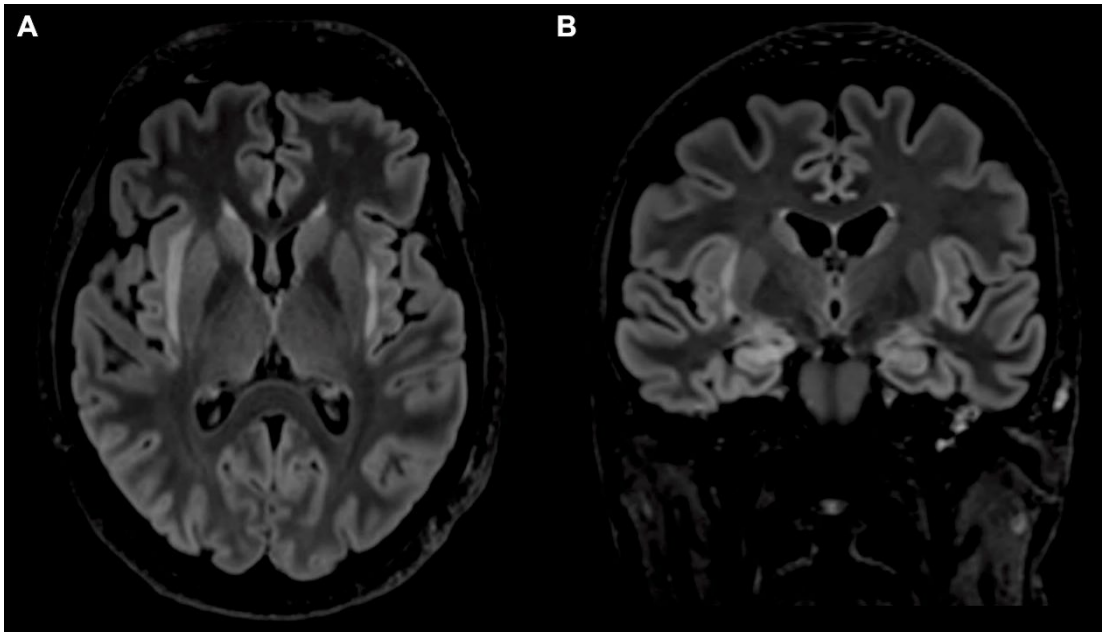

MRI (FLAIR; A, Axial; B, Coronal) performed 30 days after the onset of status epilepticus showed right-predominant hyperintensity and swelling of the claustrum, pulvinar, and hippocampus

EEG revealed bilateral or multifocal interictal epileptiform discharges and electrographic/electroclinical seizures in all patients during the long-term EEG monitoring period (example in Figure 6).

Figure 5. EEG in case 2

Bilateral asymmetric lateralized periodic discharges, predominant in the right fronto-temporal region

Patients required treatment with several antiseizure medications (ASM) (mean: 9; range: 8-10), additional antiseizure therapies (ketogenic diet, n=1; vagus nerve stimulation, n=2), anesthetics (propofol, midazolam, and ketamine, n=4 [doses detailed in Table 1]; pentothal, n=1), and immunotherapies (methylprednisolone and IVIg, n=4; plasmapheresis, n=2; anakinra, n=1; rituximab, n=1; cyclophosphamide, n=2).

Table 19. Ketamine doses used in the four patients

	Case 1	**Case 2**	**Case 3**	**Case 4**
Maximal dose	3.5 mg/kg/h	5.3 mg/kg/h	2.0 mg/kg/h	5.0 mg/kg/h
Treatment duration	22 days	15 days	15 days	40 days
Total ketamine load	135.8 g	103.8 g	44.2 g	330.0 g
Ketamine load pro kg	1636 mg/kg	1383 mg/kg	539 mg/kg	3402 mg/kg

The average duration of SE was 57 days (range: 39-90 days), while the mean duration of ICU stay was 88 days (range: 69-111 days). The only drug temporally clearly associated with SE resolution was cyclophosphamide in patient 4. Three patients experienced persistent hyperpyrexia refractory to high-dose antipyretic medications (paracetamol, diclofenac) throughout the ICU stay, despite targeted antibiotic therapies to concomitant ICU-related bacterial septicemia and pneumonia. In case 2, a primary immune regulatory disorder affecting the humoral immunity was diagnosed following SE requiring monthly immunoglobulin replacement therapy. Case 3 developed severe paraparesis likely related to a spinal cord ischemic injury occurred during the ICU stay.

In two cases (1 and 4), convulsive RSE relapsed after 12 months. In case 1, the relapse was not preceded by fever and resolved after 30 days following treatment with cyclophosphamide; the brain MRI showed new lesions of bilateral claustrum and pulvinar in the acute phase. In case 4, it was triggered by an acute tonsillitis and resolved after five days without using immunotherapies; brain MRI did not show any new lesions.

At the last follow-up of 30 ± 15 months all patients had drug-resistant epilepsy and cognitive deficits of varying severities. The mean modified Rankin scale was 2.5 (range: 2-4).

Sclerosing cholangitis

All patients developed cholestatic liver disease during their ICU stay, reversible in case 1 after reduction of ASMs, notably valproate and phenobarbital. In the three cases with persistent injury, SC involving intra- and extrahepatic bile ducts was diagnosed with MR-colangiography after 106±63 days from SE onset and was classified as secondary sclerosing cholangitis in critically ill patients (EASL et al., 2022). An example is reported in the following Figure.

Figure 6. Magnetic resonance colangiography findings in case 2

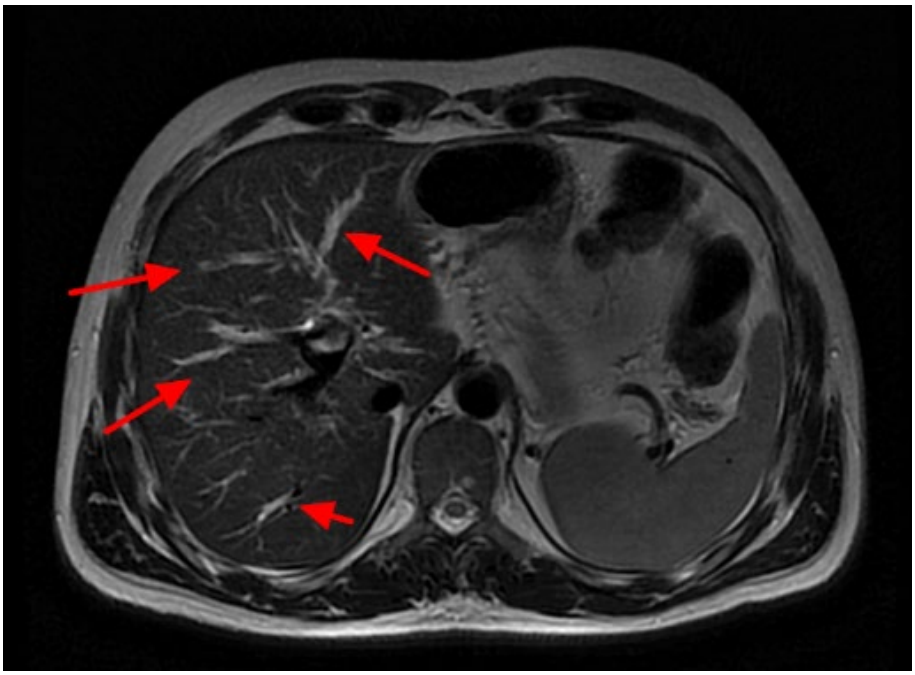

The red arrows indicate dilated bile ducts alternating with stenosis, findings consistent with sclerosing cholangitis.

ANCA and anti-IgG4 antibodies were negative. Liver blood tests were altered up to (mean ± SD): total bilirubin 8.5±3.7 mg/dL (direct>indirect), gamma-glutamyltransferase (GGT) 3012 ± 1134 U/L, alkaline phosphatase (ALP) 1169 ± 430 U/L, AST 220 ± 78 U/L, ALT 414 ± 232 U/L (Table 20); coagulation tests were normal. Cholangitis was complicated by hypercholesterolemia (n=2) and liver abscesses (n=2). All three cases are being treated with ursodeoxycholic acid (15-20 mg/kg/d) and bezafibrate, helpful in alleviating hepatobiliary injury,[7] and have preserved liver function at their last follow-up.

Table 20. Hepatobiliary assessments in the FIRES cohort

	Case 1	Case 2	Case 3	Case 4
Sclerosing cholangitis	No	Yes	Yes	Yes
MR-colangiography timing after SE onset	Not performed	49 days	75 days	194 days
*Peak bilirubin levels (direct, indirect)**	Normal	4.7 mg/dL (2.3, 2.5)	7.2 mg/dL (4.4, 2.8)	13.6 mg/dL (7.3, 6.4)
*Peak GGT levels**	910 U/L	1485 U/L	4201 U/L	3350 U/L
*Peak ALP levels**	167 U/L	748 U/L	1760 U/L	1000 U/L
*Peak AST levels**	Normal	135 U/L	324 U/L	299 U/L
*Peak ALT levels**	Normal	305 U/L	738 U/L	200 U/L
Liver abscesses	No	Yes	No	Yes

**Reference laboratory values: bilirubin total <1.2 mg/dl (direct <0.3, indirect <0.9); GGT <38 U/L; ALP <120 U/L; AST < 35 U/L; ALT <35 U/L*

Abbreviations: ALP, alkaline phosphatase; ALT, alanine aminotransferase; AST, aspartate aminotransferase; GGT, gamma-glutamiltransferase

Case 1 was found to have intrahepatic bile duct dilation on ultrasonography without SC. Despite normal laboratory exams, he remains under gastroenterological follow-up and is also being treated with ursodeoxycholic acid.

Discussion

We described four adult patients with FIRES and detailed their characteristics. Etiology remained cryptogenic despite an extensive diagnostic work-up, as typically occurs in patients with FIRES (Wickstrom et al., 2022). Regarding brain MRI findings, the most frequent alteration detected was bilateral claustrum hyperintensity, described as "claustrum sign" in patients with FIRES (Meletti et al., 2015). To date, it is unclear if this is a consequence of ictal activity or a reflection of a pathogenic mechanism affecting the same bilateral brain networks. However, because the claustrum sign has been reported also in other cytokine storm-associated disorders, including acute necrotizing encephalopathy, COVID-19-related encephalopathy, and immune effector cell-associated neurotoxicity syndrome, it may represent a specific marker of cytokine-mediated neuroinflammation (Santomasso et al., 2018; Zuhorn et al., 2020; Pensato et al., 2021; Muccioli et al., 2022). All patients were treated with several lines of

antiseizure medications and anesthetics at high dosages, as typically happens in cases of super-refractory SE. It was difficult to assess with certainty whether a drug was actually effective in resolving the SE, except for cyclophosphamide in one case, which was therefore successfully used also in the treatment of another patient of our cohort. Accordingly, cyclophosphamide was reported in other case series as effective in the management of NORSE (Kaneko et al., 2013) although it is not currently recommended in NORSE management guidelines (Wickstrom et al., 2022). All our patients were previously healthy, and developed mild to severe disabilities. Particularly, all of them had drug-resistant epilepsy and cognitive deficits at the last follow-up, as seen in about 80% of patients (Meletti et al., 2017).

Sclerosing cholangitis

A remarkable feature of our cohort, was that three out of four (75%) developed sclerosing cholangitis (SC), raising questions about a potential association between these two rare conditions. Sclerosing cholangitis (SC) is a rare chronic cholestatic biliary disease characterized by inflammation and fibrosis of the bile ducts, leading to strictures and destruction of the biliary tree, which can result in biliary cirrhosis (EASL et al., 2022). SC may be classified into primary and secondary forms. Primary SC is a presumed progressive autoimmune condition linked to inflammatory bowel disease and antineutrophilic cytoplasmic antibodies (ANCA), which can be complicated by cholangiocarcinoma (EASL et al., 2022). Secondary SC arises from identifiable injuries to the biliary system, such as prolonged biliary obstruction, infections, surgical trauma, or ischemia (Ruemmele et al., 2009; EASL et al., 2022). A newly recognized entity, SC in critically ill patients (SC-CIP), is characterized by rapid progression and has been associated with ketamine use (Martins et al., 2020; EASL et al., 2022; Leonhardt et al., 2023).

Patients with FIRES, including those in our study, require prolonged intensive care treatment, a setting where secondary SC-CIP has been recently observed with increased frequency, nevertheless remaining ultrarare (approximately 250-300 cases reported) (Martins et al., 2020). The pathogenesis of SC-CIP is characterized by ischemic colangiopathy in combination with changes in bile composition, that lead to necrosis of cholangiocytes and bile cast formation, resulting in progressive destruction and obliteration of bile ducts (Ruemmele et al., 2009; Martins et al., 2020). While

critical illness and mechanical ventilation may contribute to biliary ischemia, the hyperinflammatory state typical of FIRES might result in downregulation of hepatobiliary transporters and formation of toxic bile (Yang et al., 2009; Martins et al., 2020).

Additionally, polytherapy with ASMs, anesthetics and antipyretics at high doses over extended periods can lead to the development of drug-induced liver injury (DILI). Although DILI might be transient and resolve after drug withdrawal or dose adjustments, as observed in case 1, in a minority of patients, it can lead to bile duct injury that is visualized on imaging as SC-like changes (Ahmad et al., 2009). Ketamine is increasingly being used for the treatment of RSE (Yan et al., 2024) and has been implicated in cholangiopathy, particularly in cases of chronic abuse (Schep et al., 2023). Accordingly, the EASL Clinical Practice Guidelines on SC includes ketamine use in the differential diagnosis of SC forms (EASL 2022). Its intravenous use in the ICU has been associated with SC also in critically ill COVID-19 patients (de Tymowski et al., 2021), a condition sharing a hyperinflammatory profile with FIRES (Pensato et al., 2021). While recent forensic toxicology data challenge the notion of ketamine as a primary causative agent in SC-CIP (Leonhardt et al., 2023), it may act as a contributing factor in patients with a previously injured biliary tract due to concomitant factors, particularly when given at high doses as in our cohort.

The laboratory features of SC-CIP observed in our patients are consistent with established findings, including rapidly rising levels of GGT and ALP, along with elevated bilirubin levels - although less pronounced - while serum levels of aminotransferases are usually only mildly increased (Ruemmele et al., 2009).

As the clinical signs during the initial phase of SC-CIP are nonspecific, diagnosis is often overlooked and SC-CIP prevalence underestimated (Ruemmele et al., 2009; Martins et al., 2020). This highlights the necessity for vigilant monitoring of liver disease progression in critically ill patients, including those with FIRES, and underscores the importance of requesting a careful work-up for the differential diagnosis of SC and a MR-cholangiography in cases exhibiting persistent cholestatic injury. Timely diagnosis is crucial, as SC-CIP carries a dismal prognosis characterized by high mortality and rapid progression to liver cirrhosis (Ruemmele et al., 2009).

Medical treatment with ursodeoxycholic acid is commonly used but has limited efficacy, and endoscopic interventions allow only for palliative treatment; hence, early referral for liver transplantation should be considered for selected cases (Ruemmele et al., 2009; Martins et al., 2020).

Conclusions

Our findings suggest that patients with FIRES may be at an increased risk of developing SC-CIP, likely due to prolonged intensive care, hyperinflammation, and polytherapy with ASMs and anesthetics. Neurologists, intensivists and gastroenterologists should be aware of this possible association, as timely diagnosis of SC-CIP could significantly impact patient prognosis. Further research is needed to corroborate our findings and to clarify the role of ketamine in the pathogenesis of SC-CIP, as this may have clinical implications in the management of RSE.

CONCLUSIONS

This PhD project provides novel insights into the complex landscape of CySE, particularly through the examination of ICANS, neuro-COVID, and FIRES. By exploring biomarkers such as EEG, S100B, and NfL, this research delineates critical mechanisms underlying CySE and identifies opportunities for improving early diagnosis and intervention.

In CAR-T-associated neurotoxicity (ICANS), EEG abnormalities—specifically diffuse slowing and delta activity—were identified as early predictive markers. This finding suggests a potential clinical pathway for routine EEG monitoring to proactively identify patients at elevated risk, allowing timely intervention. The study's quantitative EEG analysis provides a structured basis for assessing CAR-T-related neurotoxicity, presenting an opportunity to refine risk stratification and develop preventative strategies, possibly reducing the impact of neurotoxicity on patient outcomes.

The neuro-COVID segment of the project revealed that NfL, but not consistently S100B, shows potential as a biomarker of neuroinflammatory damage in COVID-19, with high NfL levels correlating with both disease severity and neurological complications. This distinction highlights the complexity of using single biomarkers for predicting disease progression across cytokine storm disorders. S100B's variable results in COVID-19 point to a need for combined biomarkers or additional clinical correlates to provide a more comprehensive neuro-COVID diagnostic approach. Integrating longitudinal biomarker analysis may improve the reliability of S100B and NfL for early-stage diagnosis and risk assessment of neuro-COVID. These information may be translated and verified also in the other CySE, as a future research objective.

Lastly, the study of FIRES illustrates the devastating course of this rare condition triggered by non-specific infections, with neuroradiological markers (claustrum sign) that may represent a marker of cytokine-mediated neuroinflammation. A novel association with SSC-CIP has been described, previously reported in COVID-19 cytokine storm and likely related to persistent hyperinflammation, thus warranting liver monitoring in FIRES and other cytokine storm disorders.

Overall, this research highlights the significance of identifying biomarkers and electroclinical features in CySE and lays the groundwork for translational studies aiming to apply diagnostic and therapeutic findings across CySE. Future research should prioritize validation of multi-biomarker panels and cross-condition comparisons.

References

Abdelhak A, Barba L, Romoli M, et al. Prognostic performance of blood neurofilament light chain protein in hospitalized COVID-19 patients without major central nervous system manifestations: an individual participant data meta-analysis. J Neurol. 2023;270(7):3315-3328. doi:10.1007/s00415-023-11768-1

Aceti A, Margarucci LM, Scaramucci E, et al. Serum S100B protein as a marker of severity in Covid-19 patients. Sci Rep. 2020;10(1):18665. Published 2020 Oct 29. doi:10.1038/s41598-020-75618-0

Ahmad J, Rossi S, Rodgers SK, et al. Sclerosing Cholangitis-Like Changes on Magnetic Resonance Cholangiography in Patients With Drug Induced Liver Injury. Clin Gastroenterol Hepatol. 2019;17(4):789-790. doi:10.1016/j.cgh.2018.06.035

Alquisiras-Burgos I, Peralta-Arrieta I, Alonso-Palomares LA, Zacapala-Gómez AE, Salmerón-Bárcenas EG, Aguilera P. Neurological Complications Associated with the Blood-Brain Barrier Damage Induced by the Inflammatory Response During SARS-CoV-2 Infection. Mol Neurobiol. 2021;58(2):520-535. doi:10.1007/s12035-020-02134-7

Baig AM, Khaleeq A, Ali U, Syeda H. Evidence of the COVID-19 Virus Targeting the CNS: Tissue Distribution, Host-Virus Interaction, and Proposed Neurotropic Mechanisms. ACS Chem Neurosci. 2020;11(7):995-998. doi:10.1021/acschemneuro.0c00122

Beghi E, Michael BD, Solomon T, Westenberg E, Winkler AS, COVID-19 Neuro Research Coalition. Approaches to understanding COVID-19 and its neurological associations. Ann Neurol. 2021;89(6):1059-1067. doi:10.1002/ana.26076

Beghi E, Moro E, Davidescu EI, et al. Comparative features and outcomes of major neurological complications of COVID-19. Eur J Neurol. 2023;30(2):413-433. doi:10.1111/ene.15617

Beretta S, Cristillo V, Camera G, et al. Incidence and Long-term Functional Outcome of Neurologic Disorders in Hospitalized Patients With COVID-19 Infected With Pre-Omicron Variants. Neurology. 2023;101(9):e892-e903. doi:10.1212/WNL.0000000000207534

Beuchat I, Danish HH, Rubin DB, et al. EEG findings in CAR T-cell-associated neurotoxicity: Clinical and radiological correlations. Neuro Oncol. 2022;24(2):313-325. doi:10.1093/neuonc/noab174

Blyth BJ, Farhavar A, Gee C, et al. Validation of serum markers for blood-brain barrier disruption in traumatic brain injury. J Neurotrauma. 2009;26(9):1497-1507. doi:10.1089/neu.2008.0738

Bonetto V, Pasetto L, Lisi I, et al. Markers of blood-brain barrier disruption increase early and persistently in COVID-19 patients with neurological manifestations. Front Immunol. 2022;13:1070379. doi:10.3389/fimmu.2022.1070379

Bossuyt PM, Reitsma JB, Bruns DE, et al. STARD 2015: an updated list of essential items for reporting diagnostic accuracy studies. BMJ. 2015;351:h5527. doi:10.1136/bmj.h5527

Brisse E, Wouters CH, Matthys P. Hemophagocytic lymphohistiocytosis (HLH): A heterogeneous spectrum of cytokine-driven immune disorders. Cytokine Growth Factor Rev. 2015;26(3):263-280. doi:10.1016/j.cytogfr.2014.10.001

Butt OH, Zhou AY, Ances BM, DiPersio JF, Ghobadi A. A systematic framework for predictive biomarkers in immune effector cell-associated neurotoxicity syndrome. Front Neurol. 2023;14:1110647. doi:10.3389/fneur.2023.1110647

Buzhdygan TP, DeOre BJ, Baldwin-Leclair A, et al. The SARS-CoV-2 spike protein alters barrier function in 2D static and 3D microfluidic in-vitro models of the human blood-brain barrier. Neurobiol Dis. 2020;146:105131. doi:10.1016/j.nbd.2020.105131

Bruzzone M, Walker J, Chapin B, et al. The role of the perioperative use of EEG as a predictor/diagnostic tool for post-operative delirium: Systematic Review (P10-1.008). Neurology 2023;100(10_supplement_2) doi: 10.1212/WNL.0000000000204149

Capri M, Yani SL, Chattat R, et al. Pre-Operative, High-IL-6 Blood Level is a Risk Factor of Post-Operative Delirium Onset in Old Patients. Front Endocrinol (Lausanne). 2014;5:173. Published 2014 Oct 17. doi:10.3389/fendo.2014.00173

Cho SM, White N, Premraj L, et al. Neurological manifestations of COVID-19 in adults and children. Brain J Neurol. 2023;146(4):1648-1661. doi:10.1093/brain/awac332

de Tymowski C, Dépret F, Dudoignon E, Legrand M, Mallet V; Keta-Cov Research Group. Ketamine-induced cholangiopathy in ARDS patients. Intensive Care Med. 2021;47(10):1173-1174. doi:10.1007/s00134-021-06482-3

Edwardson, D.W., Parissenti, A.M., Kovala, A.T. (2019). Chemotherapy and Inflammatory Cytokine Signalling in Cancer Cells and the Tumour Microenvironment. In: Ahmad, A. (eds) Breast Cancer Metastasis and Drug Resistance. Advances in Experimental Medicine and Biology, vol 1152. Springer, Cham. doi:10.1007/978-3-030-20301-6_9

European Association for the Study of the Liver. Electronic address: easloffice@easloffice.eu; European Association for the Study of the Liver. EASL Clinical Practice Guidelines on sclerosing cholangitis. J Hepatol. 2022;77(3):761-806. doi:10.1016/j.jhep.2022.05.011

Fajgenbaum DC, Uldrick TS, Bagg A, et al. International, evidence-based consensus diagnostic criteria for HHV-8-negative/idiopathic multicentric Castleman disease. Blood. 2017;129(12):1646-1657. doi:10.1182/blood-2016-10-746933

Fajgenbaum DC, June CH. Cytokine Storm. N Engl J Med. 2020;383(23):2255-2273. doi:10.1056/NEJMra2026131

Freedman MS, Gnanapavan S, Booth RA, et al. Guidance for use of neurofilament light chain as a cerebrospinal fluid and blood biomarker in multiple sclerosis management. EBioMedicine. 2024;101:104970. doi:10.1016/j.ebiom.2024.104970

Grant SJ, Grimshaw AA, Silberstein J, et al. Clinical Presentation, Risk Factors, and Outcomes of Immune Effector Cell-Associated Neurotoxicity Syndrome Following Chimeric Antigen Receptor T Cell Therapy: A Systematic Review. Transplant Cell Ther. 2022;28(6):294-302. doi:10.1016/j.jtct.2022.03.006

Guasp M, Muñoz-Sánchez G, Martínez-Hernández E, et al. CSF Biomarkers in COVID-19 Associated Encephalopathy and Encephalitis Predict Long-Term Outcome. Front Immunol. 2022;13:866153. doi:10.3389/fimmu.2022.866153

Guerrero JI, Barragán LA, Martínez JD, et al. Central and peripheral nervous system involvement by COVID-19: a systematic review of the pathophysiology, clinical manifestations, neuropathology, neuroimaging, electrophysiology, and cerebrospinal fluid findings. BMC Infect Dis. 2021;21(1):515. doi:10.1186/s12879-021-06185-6

Gust J, Hay KA, Hanafi LA, et al. Endothelial Activation and Blood-Brain Barrier Disruption in Neurotoxicity after Adoptive Immunotherapy with CD19 CAR-T Cells. Cancer Discov. 2017;7(12):1404-1419. doi:10.1158/2159-8290.CD-17-0698

Gust J, Finney OC, Li D, et al. Glial injury in neurotoxicity after pediatric CD19-directed chimeric antigen receptor T cell therapy. Ann Neurol. 2019;86(1):42-54. doi:10.1002/ana.25502

Hay M, Ryan L, Huentelman M, et al. Serum Neurofilament Light is elevated in COVID-19 Positive Adults in the ICU and is associated with Co-Morbid Cardiovascular Disease, Neurological Complications, and Acuity of Illness. Cardiol Cardiovasc Med. 2021;5(5):551-565. doi:10.26502/fccm.92920221

Herlopian A, Dietrich J, Abramson JS, Cole AJ, Westover MB. EEG findings in CAR T-cell therapy-related encephalopathy. Neurology. 2018;91(5):227-229. doi:10.1212/WNL.0000000000005910

Hernani R, Aiko M, Victorio R, et al. EEG before chimeric antigen receptor T-cell therapy and early after onset of immune effector cell-associated neurotoxicity syndrome. Clin Neurophysiol. 2024;163:132-142. doi:10.1016/j.clinph.2024.04.014

Hirsch LJ, Gaspard N, van Baalen A, et al. Proposed consensus definitions for new-onset refractory status epilepticus (NORSE), febrile infection-related epilepsy syndrome (FIRES), and related conditions. Epilepsia. 2018;59(4):739-744. doi:10.1111/epi.14016

Hirsch LJ, Fong MWK, Leitinger M, et al. American Clinical Neurophysiology Society's Standardized Critical Care EEG Terminology: 2021 Version. J Clin Neurophysiol. 2021;38(1):1-29. doi:10.1097/WNP.0000000000000806

Huang X, Hussain B, Chang J. Peripheral inflammation and blood-brain barrier disruption: effects and mechanisms. CNS Neurosci Ther. 2021;27(1):36-47. doi:10.1111/cns.13569

Huby S, Gelisse P, Tudesq JJ, et al. Frontal Intermittent Rhythmic Delta Activity Is a Useful Diagnostic Tool of Neurotoxicity After CAR T-Cell Infusion. Neurol Neuroimmunol Neuroinflamm. 2023;10(4):e200111. Published 2023 Apr 14. doi:10.1212/NXI.0000000000200111

Kaneko J, Iizuka T, Asari H, et al. Retrospective Review of 6 Patients with New-Onset Refractory Status Epilepticus (NORSE) Syndrome: Early Intervention with Intravenous Cyclophosphamide May Improve Outcome. Neurology. 2013;80(7_supplement):P07.171. doi: 10.1212/WNL.80.7_supplement.P07.171

Karschnia P, Jordan JT, Forst DA, et al. Clinical presentation, management, and biomarkers of neurotoxicity after adoptive immunotherapy with CAR T cells. Blood. 2019;133(20):2212-2221. doi:10.1182/blood-2018-12-893396

Krishnan P, Glenn OA, Samuel MC, et al. Acute Fulminant Cerebral Edema: A Newly Recognized Phenotype in Children With Suspected Encephalitis. J Pediatric Infect Dis Soc. 2021;10(3):289-294. doi:10.1093/jpids/piaa063

Lee DW, Santomasso BD, Locke FL, et al. ASTCT Consensus Grading for Cytokine Release Syndrome and Neurologic Toxicity Associated with Immune Effector Cells. Biol Blood Marrow Transplant. 2019;25(4):625-638. doi:10.1016/j.bbmt.2018.12.758

Leonhardt S, Baumann S, Jürgensen C, Hüter L, Leonhardt J; Ketamine Cast Research Group. Role of intravenous ketamine in the pathogenesis of secondary sclerosing cholangitis in critically ill patients: perpetrator or innocent bystander? Answers provided by forensic toxicology. Intensive Care Med. 2023;49(12):1549-1551. doi:10.1007/s00134-023-07257-8

MacLean MA, Kamintsky L, Leck ED, Friedman A. The potential role of microvascular pathology in the neurological manifestations of coronavirus infection. Fluids Barriers CNS. 2020;17(1):55. doi:10.1186/s12987-020-00216-1

Marchi N, Angelov L, Masaryk T, et al. Seizure-promoting effect of blood-brain barrier disruption. Epilepsia. 2007;48(4):732-742. doi:10.1111/j.1528-1167.2007.00988.x

Marchi N, Rasmussen P, Kapural M, et al. Peripheral markers of brain damage and blood-brain barrier dysfunction. Restor Neurol Neurosci. 2003;21(3-4):109-121

Marchi N, Cavaglia M, Fazio V, Bhudia S, Hallene K, Janigro D. Peripheral markers of blood-brain barrier damage. Clin Chim Acta Int J Clin Chem. 2004;342(1-2):1-12. doi:10.1016/j.cccn.2003.12.008

Martins P, Verdelho Machado M. Secondary Sclerosing Cholangitis in Critically Ill Patients: An Underdiagnosed Entity. GE Port J Gastroenterol. 2020;27(2):103-114. doi:10.1159/000501405

Meletti S, Slonkova J, Mareckova I, et al. Claustrum damage and refractory status epilepticus following febrile illness. Neurology. 2015;85(14):1224-1232. doi:10.1212/WNL.0000000000001996

Meletti S, Giovannini G, d'Orsi G, et al. New-Onset Refractory Status Epilepticus with Claustrum Damage: Definition of the Clinical and Neuroimaging Features. Front Neurol. 2017;8:111. Published 2017 Mar 27. doi:10.3389/fneur.2017.00111

Morris EC, Neelapu SS, Giavridis T, Sadelain M. Cytokine release syndrome and associated neurotoxicity in cancer immunotherapy. Nat Rev Immunol. 2022;22(2):85-96. doi:10.1038/s41577-021-00547-6

Muccioli L, Pensato U, Cani I, Guarino M, Cortelli P, Bisulli F. COVID-19-Associated Encephalopathy and Cytokine-Mediated Neuroinflammation. Ann Neurol. 2020;88(4):860-861. doi:10.1002/ana.25855

Muccioli L, Pensato U, Di Vito L, Messia M, Nicodemo M, Tinuper P. Teaching NeuroImage: Claustrum Sign in Febrile Infection-Related Epilepsy Syndrome. Neurology 2022;98/10):e1090-e1091. 10.1212/WNL.0000000000013261

Needham EJ, Ren AL, Digby RJ, et al. Brain injury in COVID-19 is associated with dysregulated innate and adaptive immune responses. Brain J Neurol. 2022;145(11):4097-4107. doi:10.1093/brain/awac321

Neelapu SS, Tummala S, Kebriaei P, et al. Chimeric antigen receptor T-cell therapy - assessment and management of toxicities. Nat Rev Clin Oncol. 2018;15(1):47-62. doi:10.1038/nrclinonc.2017.148

Neilson DE, Adams MD, Orr CM, et al. Infection-triggered familial or recurrent cases of acute necrotizing encephalopathy caused by mutations in a component of the nuclear pore, RANBP2. Am J Hum Genet. 2009;84(1):44-51. doi:10.1016/j.ajhg.2008.12.009

Ousseiran ZH, Fares Y, Chamoun WT. Neurological manifestations of COVID-19: a systematic review and detailed comprehension. Int J Neurosci. 2023;133(7):754-769. doi:10.1080/00207454.2021.1973000

Park JH, Nath K, Devlin SM, et al. CD19 CAR T-cell therapy and prophylactic anakinra in relapsed or refractory lymphoma: phase 2 trial interim results. Nat Med. 2023;29(7):1710-1717. doi:10.1038/s41591-023-02404-6

Pensato U, Muccioli L, Cani I, Janigro D, Zinzani PL, Guarino M, Cortelli P, Bisulli F. Brain dysfunction in COVID-19 and CAR-T therapy: cytokine storm-associated encephalopathy. Ann Clin Transl Neurol 2021;8(4):968-979. doi:10.1002/acn3.51348

Pensato U, Amore G, Muccioli L, et al. CAR t-cell therapy in BOlogNa-NEUrotoxicity TReatment and Assessment in Lymphoma (CARBON-NEUTRAL): proposed protocol and results from an Italian study. J Neurol. 2023;270(5):2659-2673. doi:10.1007/s00415-023-11595-4

Perrin P, Collongues N, Baloglu S, et al. Cytokine release syndrome-associated encephalopathy in patients with COVID-19. Eur J Neurol. 2021;28(1):248-258. doi:10.1111/ene.14491

Ponten SC, Tewarie P, Slooter AJ, Stam CJ, van Dellen E. Neural network modeling of EEG patterns in encephalopathy. J Clin Neurophysiol. 2013;30(5):545-552. doi:10.1097/WNP.0b013e3182a73e16

Ravelli A, Minoia F, Davì S, et al. 2016 Classification Criteria for Macrophage Activation Syndrome Complicating Systemic Juvenile Idiopathic Arthritis: A European League Against Rheumatism/American College of Rheumatology/Paediatric Rheumatology International Trials Organisation Collaborative Initiative. Arthritis Rheumatol. 2016;68(3):566-576. doi:10.1002/art.39332

Remsik J, Wilcox JA, Babady NE, et al. Inflammatory Leptomeningeal Cytokines Mediate COVID-19 Neurologic Symptoms in Cancer Patients. Cancer Cell. 2021;39(2):276-283.e3. doi:10.1016/j.ccell.2021.01.007

Rubin DB, Al Jarrah A, Li K, et al. Clinical Predictors of Neurotoxicity After Chimeric Antigen Receptor T-Cell Therapy. JAMA Neurol. 2020;77(12):1536-1542. doi:10.1001/jamaneurol.2020.2703

Ruemmele P, Hofstaedter F, Gelbmann CM. Secondary sclerosing cholangitis. Nat Rev Gastroenterol Hepatol. 2009;6(5):287-295. doi:10.1038/nrgastro.2009.46

Sahin BE, Celikbilek A, Kocak Y, Saltoglu GT, Konar NM, Hizmali L. Plasma biomarkers of brain injury in COVID-19 patients with neurological symptoms. J Neurol Sci. 2022;439:120324. doi:10.1016/j.jns.2022.120324

Santomasso BD, Park JH, Salloum D, et al. Clinical and Biological Correlates of Neurotoxicity Associated with CAR T-cell Therapy in Patients with B-cell Acute

Lymphoblastic Leukemia. Cancer Discov. 2018;8(8):958-971. doi:10.1158/2159-8290.CD-17-1319

Schep LJ, Slaughter RJ, Watts M, Mackenzie E, Gee P. The clinical toxicology of ketamine. Clin Toxicol (Phila). 2023;61(6):415-428. doi:10.1080/15563650.2023.2212125

Solomon T. Neurological infection with SARS-CoV-2 - the story so far. Nat Rev Neurol. 2021;17(2):65-66. doi:10.1038/s41582-020-00453-w

Sterner RC, Sterner RM. CAR-T cell therapy: current limitations and potential strategies. Blood Cancer J. 2021;11(4):69. Published 2021 Apr 6. doi:10.1038/s41408-021-00459-7

Strati P, Jallouk A, Deng Q, et al. A phase 1 study of prophylactic anakinra to mitigate ICANS in patients with large B-cell lymphoma. Blood Adv. 2023;7(21):6785-6789. doi:10.1182/bloodadvances.2023010653

Taruffi L, Muccioli L, Mitolo M, et al. Neurological Manifestations of Long COVID: A Single-Center One-Year Experience. Neuropsychiatr Dis Treat. 2023;19:311-319. doi:10.2147/NDT.S387501

Undén L, Calcagnile O, Undén J, Reinstrup P, Bazarian J. Validation of the Scandinavian guidelines for initial management of minimal, mild and moderate traumatic brain injury in adults. BMC Med. 2015;13:292. Published 2015 Dec 9. doi:10.1186/s12916-015-0533-y

Wang SY, Chen W, Xu W, et al. Neurofilament Light Chain in Cerebrospinal Fluid and Blood as a Biomarker for Neurodegenerative Diseases: A Systematic Review and Meta-Analysis. J Alzheimers Dis. 2019;72(4):1353-1361. doi:10.3233/JAD-190615

Webb BJ, Peltan ID, Jensen P, et al. Clinical criteria for COVID-19-associated hyperinflammatory syndrome: a cohort study. Lancet Rheumatol. 2020;2(12):e754-e763. doi:10.1016/S2665-9913(20)30343-X

Wickstrom R, Taraschenko O, Dilena R, et al. International consensus recommendations for management of New Onset Refractory Status Epilepticus (NORSE) incl. Febrile Infection-Related Epilepsy Syndrome (FIRES): Statements and Supporting Evidence. Epilepsia. 2022. doi:10.1111/epi.17397

Williams GW, Lüders HO, Brickner A, Goormastic M, Klass DW. Interobserver variability in EEG interpretation. Neurology. 1985;35(12):1714-1719. doi:10.1212/wnl.35.12.1714

Yan M, Sun T, Liu J, Chang Q. The efficacy and safety of ketamine in the treatment of super-refractory status epilepticus: a systematic review. J Neurol. 2024;271(7):3942-3952. doi:10.1007/s00415-024-12453-7

Yanagida A, Kanazawa N, Kaneko J, et al. Clinically based score predicting cryptogenic NORSE at the early stage of status epilepticus. Neurol Neuroimmunol Neuroinflamm. 2020;7(5):e849. Published 2020 Jul 29. doi:10.1212/NXI.0000000000000849

Yang H, Plösch T, Lisman T, et al. Inflammation mediated down-regulation of hepatobiliary transporters contributes to intrahepatic cholestasis and liver damage in murine biliary atresia. Pediatr Res. 2009;66(4):380-385. doi:10.1203/PDR.0b013e3181b454a4

Zhou F, Yu T, Du R, et al. Clinical course and risk factors for mortality of adult inpatients with COVID-19 in Wuhan, China: a retrospective cohort study [published correction appears in Lancet. 2020 Mar 28;395(10229):1038. doi: 10.1016/S0140-6736(20)30606-1] [published correction appears in Lancet. 2020 Mar 28;395(10229):1038. doi: 10.1016/S0140-6736(20)30638-3]. Lancet. 2020;395(10229):1054-1062. doi:10.1016/S0140-6736(20)30566-3

Zingaropoli MA, Iannetta M, Piermatteo L, et al. Neuro-Axonal Damage and Alteration of Blood-Brain Barrier Integrity in COVID-19 Patients. Cells. 2022;11(16):2480. doi:10.3390/cells11162480

Zuhorn F, Omaimen H, Ruprecht B, et al. Parainfectious encephalitis in COVID-19: "The Claustrum Sign". J Neurol. 2021;268(6):2031-2034. doi:10.1007/s00415-020-10185-y